Since January 2020 Elsevier has created a COVID-19 resource centre with free information in English and Mandarin on the novel coronavirus COVID-19. The COVID-19 resource centre is hosted on Elsevier Connect, the company's public news and information website.

Composites Part A 137 (2020) 106009

Contents lists available at ScienceDirect

Composites Part A

journal homepage: www.elsevier.com/locate/compositesa

Review

Structural design and environmental applications of electrospun nanofibers

Wenshuo Zhang[1], Ziying He[1], Ying Han, Qinyuan Jiang, Chenhao Zhan, Kaiji Zhang, Zekun Li, Rufan Zhang*

Beijing Key Laboratory of Green Chemical Reaction Engineering and Technology, Department of Chemical Engineering, Tsinghua University, Beijing 100084, China

ARTICLE INFO

Keywords:
Nanofibers
Electrospinning
Environmental applications
Self-cleaning

ABSTRACT

Nanofibers have attracted extensive attention and been applied in various fields due to their high aspect ratio, high specific surface area, flexibility, structural abundance, *etc*. The electrospinning method is one of the most promising and effective ways to produce nanofibers. The electrospun nanofibers-based films and membranes have already been demonstrated to possess small pore sizes, larges specific surface area, and can be grafted with different functionalities to adapt to various purposes. The environmental applications of nanofibers are one of the essential application fields, and great achievements have been made in this field. To well summarize the development of nanofibers and their environmental applications, we review the nanofiber fabrication methods, advanced fiber structures, and their applications in the field of air filtration, heavy metal removal, and self-cleaning surface. We hope this review and summary can provide readers a comprehensive understanding of the structural design and environmental applications of electrospun nanofibers.

1. Introduction

As severe global problems nowadays, environmental pollutions are seriously threatening human beings' health and economic development. The contaminations in air, water, and soil, *etc*., cause many health problems such as allergy, cardiovascular disorder, and infant mortality. According to the investigation published in 2017 by The Lancet Commission on pollution and health, about nine million premature deaths in the whole world were considered to associate with environmental pollutions only in 2015. Notably, about 6.5 million deaths were considered to result from air pollution, and 1.8 million deaths were linked to water pollution. As is known, air pollution usually occurs when excessive amounts of noxious substances enter the earth's atmosphere [1]. Air pollution sources include gases (such as ammonia [2–4] and carbon monoxide [5,6]), suspending organic/inorganic particulate matters (PM) [7–9], biological molecules, *etc.*, all of which can cause direct damage to the atmosphere. Besides, water pollution is another severe problem that human beings are facing nowadays. The industrial effluents have already caused severe water pollution due to the heavy metal ions in the water supplies or toxic waste [10]. For example, poor water qualities were reported in Evanston in the U. S. since the toxic chromium (Cr (VI)) was found in the drinking water supplies in 2011.

Tremendous efforts have been made to protect natural environments and to reduce air and water pollution, such as setting up more strict industrial emission regulations, developing electric vehicles, and producing more sustainable power supplies. Among all the efforts to protect natural environments, removing pollutants directly from the air emits or polluted water is undoubtedly one of the most effective methods. Numerous novel techniques are developed based on such purpose, and some of them have already been successfully applied in our daily life or industrial fields. The most common and widely-used devices in daily life are portable air filters and active carbon-based in-house water purifiers. Conventional materials or devices used for filtration or purification usually have some shortages, such as low adsorption efficiency, small capacity, limited durability, and lack of reusability. In contrast, functional nanofiber membranes draw considerable attention in recent years due to their excellent properties to overcome the conventional limitations mentioned earlier. There are many ways to fabricate functional nanofiber mats, such as self-assembly [11–13], melt-blowing [14–16], ultrasonically-blowing [17,18], solution blowing [19–21], electrospinning [22,23], and direct blow-spinning [24,25]. Among all the above methods for producing nanofibers, electrospinning is considered as a very effective one and has been widely adopted for both academic and industrial applications. Electrospun nanofibers show many advantages for filtration and purification because of their tiny fiber diameters, large specific areas, strong adhesion towards PM particles, abundant pores, tunable structures, simple chemical modifications, and low costs, *etc*. Therefore, functional

* Corresponding author.
E-mail address: zhangrufan@tsinghua.edu.cn (R. Zhang).
[1] These two authors contributed equally to this work.

https://doi.org/10.1016/j.compositesa.2020.106009
Received 9 April 2020; Received in revised form 27 May 2020; Accepted 8 June 2020
Available online 12 June 2020
1359-835X/

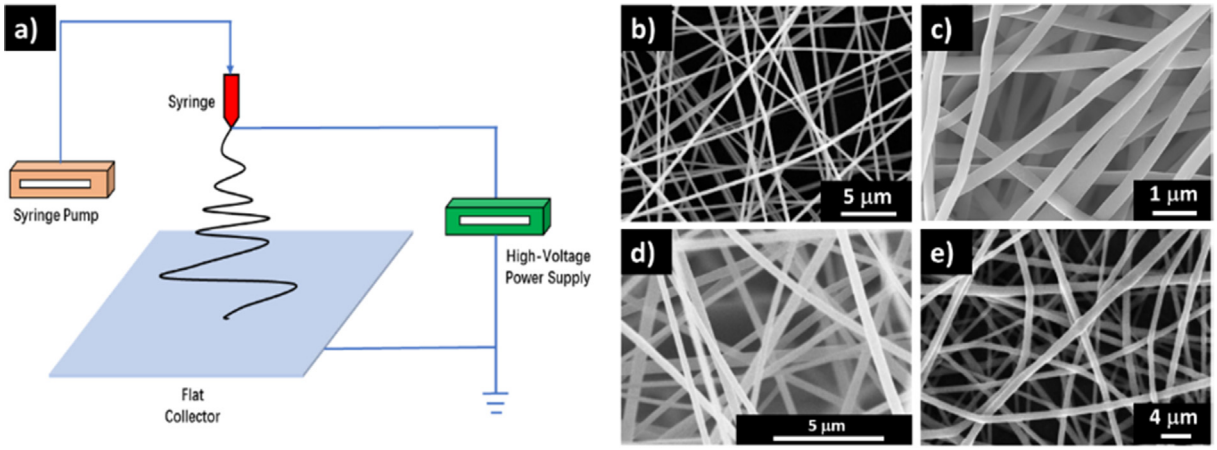

Fig. 1. a) Schematic of a basic electrospinning setup. b) Polyimide (PI) nanofibers prepared *via* PI/dimethylformamide (DMF) solution [57]. Reproduced with permission from [57], Copyright 2016, American Chemical Society. c) Polyacrylonitrile (PAN) nanofiber *via* 8 wt% PAN/DMF solution [58]. Reproduced with permission from [58], Copyright 2017, Elsevier. d) Cellulose acetate (CA) nanofibers prepared *via* 19 wt% CA /DMF/acetone solution [59]. Reproduced with permission from [59], Copyright 2020, Elsevier. (e) Polylactic acid (PLA) nanofibers prepared *via* 10 wt% PLA /DMF/chloroform solution [60]. Reproduced with permission from [60], Copyright 2019, Elsevier. (For interpretation of the references to colour in this figure legend, the reader is referred to the web version of this article.)

electrospun nanofibers have already been applied in biomedical and environmental applications, such as tissue engineering [26–28], biomaterials [29–31], energy storage [32–34], drug delivery & releasing [35–37], and environmental protection [38–40], *etc*.

In this work, we review the experimental setup, mechanisms, structural design, effecting parameters of the basic electrospinning method, which is used to fabricate solid nanofibers. In the meanwhile, three types of nanofibers with advanced structures (core–shell, alignment, and hollow) and the corresponding fabrication methods are introduced. Then, we summarize the environmental applications of electrospun nanofibers in air filtration, heavy metal ions adsorption process for water purification purposes, and self-cleaning applications. We review the applying mechanism and recent experimental approaches for the development of each application. Finally, we give our conclusions and outlooks in this field.

2. Fabrication of electrospun nanofibers

As a promising and effective procedure to continuously produce nanofibers, Formhals issued the first electrospinning US patent in 1934 [41]. Electrospinning can be classified into two categories based on the types of spinning substances, *i.e.*, solvent electrospinning and melt electrospinning. Here, in this review, the spinning materials and experimental progress are focused on solvent electrospinning unless melt electrospinning process is specified.

2.1. Polymeric materials and solvents

A wide range of polymers can be used for electrospinning and forming various nanofibers with tunable sizes for different applications. The polymers used for fabricating electrospun nanofibers can be classified into two genres, *i.e.*, natural polymers, and synthetic polymers. Natural polymers indicate the polymeric materials that occur in nature or derivations from natural origins. For instance, collagen [23,42,43], gelatin [44–46], soy protein [47,48], silk [29], cellulose [49], and chitosan [50] belong to natural polymers. Natural polymers are found to be environmentally benign and beneficial for the development of tissue engineering [51], biodiesels, and chemical industry, *etc*. Synthetic polymers refer to human-made polymers derived from petroleum products, which include common polymers such as polyester, Teflon, nylon, polyvinyl chloride (PVC), and polyacrylonitrile (PAN) [52]. Synthetic polymers are widely used in industries and households. The typical applications include Teflon served in non-stick cookware, nylons in textiles, and PVC in pipes, *etc*. The polymers are usually dissolved in proper solvents to form solutions for electrospinning. Common solvents include water, ethanol, chloroform, dimethylformamide (DMF), and tetrahydrofuran (THF), *etc*. The polymers used for electrospinning method need to be soluble in solvents and their molecular weight need to be large enough to allow polymer chains to entangle during the electrospinning process. Generally, the selected polymeric materials will be mixed with proper solvents and stirred at the desired operating temperature for a sufficient time to completely dissolve the polymers. Different combinations of polymers and solvents serve for different purposes. For example, PAN and DMF solutions are applied for fabricating PAN nanofibers and enhancing the heat transfer rate in pool boiling [17]. Polystyrene (PS) and tetrahydrofuran (THF) solutions are utilized for the research of ion exchange [53]. PLGA, a copolymer of poly (glycolic acid) (PGA) and polylactic acid (PLA), was mixed with chloroform and DMF solvents and used to investigate the interactions between cells and nanofibers for bone regeneration [54]. Chitosan and TiO_2 nanoparticles are mixed in acetic acid to test the nanofiber adsorbability of heavy metal ions [55].

2.2. Basic electrospinning setup and fabrication process

Generally, electrospinning is conducted at room temperature and under atmospheric pressure. The basic electrospinning setup depicted in Fig. 1a usually consists of four parts, *i.e.*, spinneret, fiber collector, high-voltage power supply and flow control pump. A plastic syringe with a metallic needle is used as a spinneret. A metallic needle is attached to the syringe and act as an electrode. A collector connects to the applied voltage and acts as the counter electrode. The distance between the collector (the counter electrode) and the spinneret tip (primary electrode) varies according to experimental parameters. In the basic electrospinning setup, the collector is usually placed 10–25 cm away from the needle tip and has a variety of configurations. The high-voltage power supply provides an electrostatic field between two electrodes. The provided power usually ranges from 10 kV to 50 kV. The plastic syringe, which is filled up with prepared polymer solutions, is installed on the flow control pump. The pump adjusts the flow rate of polymer solutions, which varies from microliters per hour to milliliters per hour, depending on the solution viscosity and the spinneret size.

When a polymer solution is charged with high voltage, the electrostatic field between the electrodes immediately imposes an electric

Maxwell stress onto the solution droplet. The imposed stress deforms the droplet into a cone shape, which is known as Taylor cone, and initiates an electrospinning process [56]. Once a solution jet is initiated, it will be immediately stretched into a long and thin filament due to the drag force. After a short straight part, the jet experiences bending instability, splitting process, and fast solvent evaporation process. Finally, the jet forms into one or many long and thin filaments, which depends on the properties of polymer solutions and other parameters. The resulting fiber size ranges from nanometers to several microns. Randomly orientated fibers are collected on a grounded collector. Scanning electron microscopy (SEM) images of solid electrospun nanofibers produced from different combinations of polymer and solvent are shown in Figs. 1b-1e.

2.3. Effecting parameters

Fiber formations and morphologies are largely affected by experimental parameters, including the applied voltage [61,62], distance between the two electrodes [63], and the solution flow rate [64], *etc*. Furthermore, the solution conductivity [65,66], solution viscosity [67], humidity [68–70], and temperature [71–73], *etc*., are also important factors. The impact of these parameters on electrospinning is briefly summarized in Table 1.

The applied voltage is a critical parameter for fiber formation. The charged jets ejected from the Taylor cone only occur when the applied voltage exceeds the threshold voltage. Otherwise, the solution droplet will suspend on the spinneret if the provided voltage is inadequate. The properties of the electrospinning solution determine the values of the threshold voltage. The effects of the applied voltage on the fiber morphologies are complicated. For example, it had been reported by Doshi and Reneker that the radius of polyethylene oxide (PEO) nanofibers did not show clear responses to the changing applied voltage [74], while Bakar *et al.* reported that the diameter of PAN nanofibers increased with the voltage increase [75]. Thus, it is still in debate regarding the general effects of the applied voltage to fiber morphologies. The flow rate determines the solution feedstock to the spinneret. A slow flow rate may result in polymer solidification inside the spinneret tip, which thus cannot form into a Taylor cone. In contrast, the solutions will drip from the spinneret tip at a fast pumping rate. Within an appropriate range, the impact of the solution flow rate on the fiber morphologies is evident. Any increase of feeding rate leads to the enlarged diameter of the electrospun fibers [76,77]. The distance between spinneret and collector is another crucial parameter to determine the fiber morphologies. Increasing the distance will contribute to the increased jets traveling time and solvent evaporation time. Therefore, thinner fibers can be collected if the distance between electrodes is increased. However, it should be noticed that such phenomena will only occur when the working distance does not exceed an appropriate range [75,78].

2.4. Electrospun nanofibers with unique structures

Solid nanofibers can be fabricated *via* primary electrospinning processes and have been applied in many areas. However, solid nanofibers and basic fabrication processes cannot fulfill the growing requests for advanced nanofibers. It is always in great demand that nanofibers have more wanted properties such as higher qualities, more functionalities, larger surface areas, high permeability, and porosity. Thus, several modifications have been made to the basic setup, and advanced fiber structures have been developed. The improvement mainly focuses on fiber deposited orientations and fiber morphologies. Three types of specially-designed nanofibers, including aligned nanofibers, core–shell nanofibers, and hollow nanofibers, are summarized below. These fiber morphologies are closely related to the environmental applications of electrospun nanofibers.

2.4.1. Aligned nanofibers

Electrospun nanofibers usually deposit randomly on collectors and form nonwoven mats. The first design to fabricate electrospun nanofibers with uniaxial orientation was reported in 2001 [81]. This experimental setup still employed some necessary facilities: a single-compartment spinneret, a syringe pump, and a high voltage supply. Here, a rotating disc with a sharpened edge of 53.2° was utilized as the fiber collector. Controlling the fiber orientations on collectors and arranging them into desired alignments are of great significance and extensive application potential. Since well-aligned or highly ordered nanofibers exhibit enhanced performance. For instance, aligned polylactic acid (PLLA) electrospun nanofibers facilitated the phosphorylation of mesenchymal stem cells [82] and contributed 8.11% efficiency enhancement for capturing cancer cells [60]. Therefore, fiber orientation improvement has attracted worldwide attention. The specific expectations are found in fields such as biomedicine, tissue engineering, and composite reinforcement. Fabricating aligned electrospun nanofibers is challenging due to unstable and intervened polymer jets. So far, the efforts regarding fiber alignments include modifying collectors, changing experimental processes, and adding extra forces.

Collectors used in the basic electrospinning process are grounded conductive plates. It is feasible to reduce the jet inventions and enhance the alignment degree by using modified collectors. So far, the collectors used to collect aligned fibers can be categorized into two types: rotating and parallel. A typical rotating collector is a copper wire-framed drum, which is composed of two circular nonconducting disks and several connecting PVC pipes (Fig. 2a) [83]. The fiber orientations on this configuration were driven by electrostatic interactions, which include i) the electrostatic force generated by the applied electric field, and ii) the forces between the charged incoming fibers and the ones attached to the collector. The degree of fiber alignment depends on the rotating speed of the drum. Moreover, Zhao *et al.* utilized parallel electrodes to collect polyvinyl alcohol (PVA) nanofibers [84]. The gap between two parallel electrodes served as a fiber collector. This configuration could form a positively charged ring between the spinneret and two parallel

Table 1
The solution and surroundings effects on the formation and morphologies of electrospun nanofibers.

Parameters	Impact on electrospinning	Reference
Conductivity	Increasing solution conductivity can facilitate the jet stretching, reducing the bead forming possibilities and fiber diameter, resulting in the improvement of fiber quality	[66,66,79]
Viscosity	High solution viscosity leads to insufficient strength to stretch jets into fibers; jets will break into droplets directly, and no fibers will form if the viscosity is too low	[67]
Surface tension	Reducing surface tension contributes to smooth fiber morphologies	[80]
Solvent volatility	Generally, the volatile solvent can evaporate rapidly and facilitate the jet solidification; too high volatile solvent may lead to the quick block of the needle tip.	[80]
Humidity	High surrounding humidity may prevent the solvent evaporation during the jet solidification process and lead to undesirable fiber morphologies; such effect depends on the employed polymer.	[68–70]
Temperature	Increasing the surrounding temperature will increase the solvent evaporation rate and reduce the solution viscosity simultaneously, and result in the decreasing fiber diameter.	[71–73]

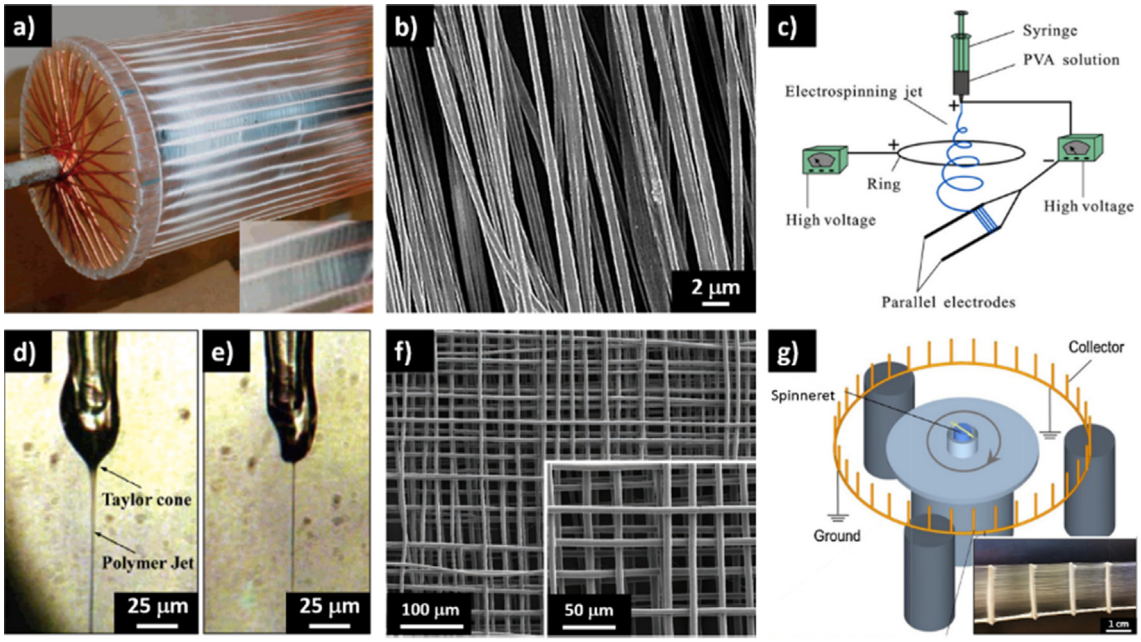

Fig. 2. a) A rotating copper wire-framed drum used to collect aligned electrospun nanofibers [83]. Reproduced with permission from [83], Copyright 2004, American Chemical Society. b) SEM images of aligned electrospun nanofibers [84]. c) Schematic of alignment electrospinning by using parallel electrodes as a fiber collector [84]. Reproduced with permission from [84], Copyright 2016, Elsevier. d)-e) Polymer jets erupted from the NFES system [88]. Reproduced with permission from [88], Copyright 2006, American Chemical Society. f) Highly crossed nanofibers fabricated *via* melt electrospinning [90]. Reproduced with permission from [90], Copyright 2011, John Wiley and Sons. g) Schematic of centrifugal electrospinning [92]. Reproduced with permission from [92], Copyright 2015, Elsevier. (For interpretation of the references to colour in this figure legend, the reader is referred to the web version of this article.)

electrodes. Electrostatic force stretched unstable filaments and resulted in highly aligned electrospun nanofibers (Fig. 2b and 2c) [80]. Furthermore, a flowing water bath [85], a piece of concaved aluminum [86], and even an insulating tube [87] can also serve as a collector to improve the fiber alignments.

Another approach to controlling fiber orientation is changing experimental parameters. The random fiber deposition on a collector is caused by jet bending instability. Near-field electrospinning technique (NFES) was developed to overcome the drawback of jet instability (Fig. 2d and 2e) and was considered as an effective and secure method to control fiber deposition. This technique reduces the applied electrostatic voltage, employs a much smaller spinneret, and tremendously shortens the distance between spinneret and collector. These modifications are trying to utilize stable jet regions (500 μm to 3 mm) [88]. By employing NFES, individual fiber deposition on a planar silicon substrate can be precisely controlled [89]. Melt electrospinning employs a writing pattern to enhance fiber alignments. By controlling the collector moving speed and direction, Brown *et al.* fabricated a sophisticated fiber deposition pattern *via* melt electrospinning technique [90] (Fig. 2f). The developed precise deposition method demonstrated that melt electrospinning nanofibers could be used as scaffolds and considered as an additional option for the current additive manufacturing (AM) technology.

Adopting extra forces can also prepare well-aligned nanofiber arrays. For instance, a centrifugal electrospinning (CES) system is demonstrated to be effective in producing highly aligned nanofibers (Fig. 2g). A horizontal, rotating spinneret is utilized to replace the stationary vertical one in the basic spinning system. CES employes electrostatic and centrifugal force simultaneously. For example, Edmondson *et al.* successfully fabricated highly aligned polyvinylidene fluoride (PVDF) nanofibers *via* CES. They also reported that the alignment degree of nanofibers could be improved by increasing the spinneret rotating speed [91]. Furthermore, Erickson *et al.* employed CES to fabricate chitosan and polycaprolactone (PCL) co-polymeric nanofibers, which possessed highly aligned pattern and relatively large surface area [92]. Moreover, an extra magnetic field can assist the fabrication of highly aligned nanofibers. A magnetic-field-assisted electrospinning (MFAES) system still employs a vertical stationary spinneret, while two magnets are added onto the planar collector. By utilizing this simple modification, Mei *et al.* prepared highly aligned PAN/polyvinylpyrrolidone (PVP)/multiwalled carbon nanotubes (MWCNTs) nanofibers. Meanwhile, it had been found that higher concentration of MWCNTs and lower applied voltage could contribute to higher fiber alignments [93].

2.4.2. Core-shell nanofibers

Electrospun nanofibers fabricated *via* basic setup have been demonstrated to be effective in many fields. However, the solid structure of nanofiber and spinning material requirements have limited their applications in areas such as drug-releasing and tissue engineering. Special additives may lose activities during the fabrication processes of solid nanofibers in normal electrospinning processes. In contrast, core–shell nanofibers can encapsulate functional agents inside the core and sustain their activities in the meanwhile. Besides, the core–shell structure allows specific components to be imparted onto the fiber shell and does not weaken the core functionalities. Furthermore, core–shell nanofibers enable many unspinnable polymers to be utilized as electrospinnable materials. Therefore, core–shell electrospun nanofibers have attracted wide attention and been studied with various materials and purposes. For instance, Lee *et al.* employed self-healing transparent core–shell nanofibers for anti-corrosive protections. They used PAN as the shell and dimethyl-methyl hydrogen-siloxane as the core [94]. Mickova *et al.* reported a type of core–shell nanofibers with embedded liposomes. These fibers utilized polyvinyl alcohol (PVA) as the core and poly-ε-caprolactone as the shell. The inside enzymatic activities were well preserved [95].

Core-shell nanofibers can be fabricated *via* several methods, such as multistep template synthesis, chemical deposition, and coaxial electrospinning. Among these approaches, coaxial electrospinning is considered as a versatile method to fabricate core–shell nanofibers. Coaxial

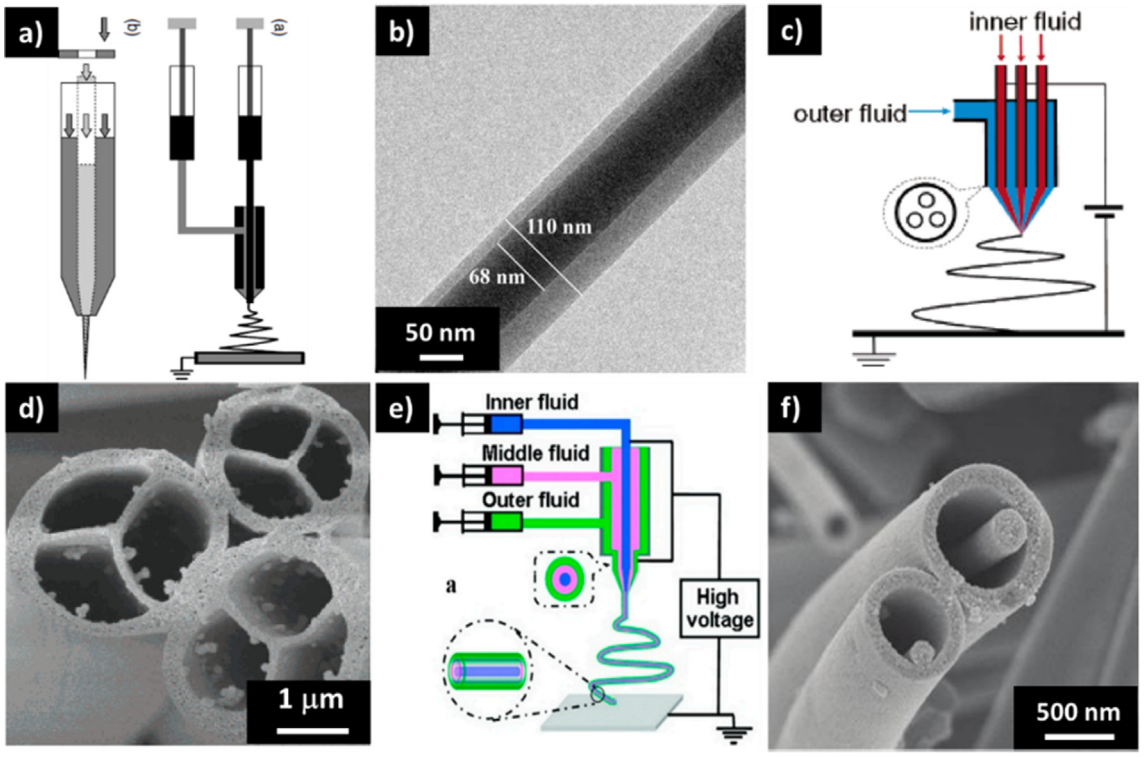

Fig. 3. a) Spinnenet used for coaxial electrospinning, two separate syringes (upper) and a double-compartment spinneret (bottom) [97]. Reproduced with permission from [97], Copyright 2012, Elsevier. b) Core-shell structured electrospun nanofiber [98]. Reproduced with permission from [98], Copyright 2016, Elsevier. c) Triple-compartment spinneret used in triaxial electrospinning [99]. d) Multichannel electrospun nanofibers [99]. Reproduced with permission from [99], Copyright 2010, American Chemical Society. e) Spinneret with a concentric structure [100]. f) Multiwalled electrospun nanofibers [100]. Reproduced with permission from [100], Copyright 2007, American Chemical Society. (For interpretation of the references to colour in this figure legend, the reader is referred to the web version of this article.)

electrospinning was firstly developed in 2003 [96]. Such development was inspired by traditional fields, like the melt spinning of core–shell structured fibers [56]. The setup of coaxial electrospinning still employs a high-voltage power supply, a flow control pump, and a nanofiber collector. Instead of using a single-compartment spinneret, two separate syringes or a double-compartment syringe are utilized. This unique design allows two solutions simultaneously following in the same nozzle (Fig. 3a) [97]. The mechanism of co-electrospinning is similar to the common electrospinning. When a direct current (DC) electric field is applied between the spinneret and the ground collector, a core–shell droplet transforms into a cone shape. It also contains processes such as jet thinning, solvent evaporating, and jet stretching. Finally, the core–shell nanofibers are formed and collected by a grounded collector (Fig. 3b) [56,98]. Polymers used for coaxial electrospinning require similar dielectric properties. The further modification of coaxial electrospinning is triaxial electrospinning, in which three polymer solutions are provided to the spinneret. Currently, two main types of spinnerets are used for triaxial electrospinning : (i) a triple-compartments spinneret and (ii) a concentric spinneret using three separate syringes. Nanofibers with three independent channels can be obtained by the former spinneret (Fig. 3c and 3d), while the latter case will result in nanofibers with a core–shell-shell structure (Fig. 3e and 3f) [99,100].

The nanofiber morphologies and mechanical properties can be adjusted by changing experimental parameters in coaxial electrospinning. For example, Chen *et al.* reported that changing the feeding ratio of two polymers could modify the core–shell structure. This work fabricated heparin/poly (L-lactic acid-co-ε-caprolactone) [P(LLA-CL)] core–shell nanofibers *via* coaxial electrospinning method. By increasing the feeding ratio of core and shell solution from 1:3 to 1:2, the diameter of the fiber core was increased from ~90 nm to ~180 nm. As the feeding ratio was increased to 1:1, strings with beads formed [101]. Besides, the miscibility of the core and shell solution is another factor that tremendously influences the coaxial electrospinning process. It was reported that two immiscible core and shell components could fabricate well-defined core/shell structure. Partially miscible solutions will lead to the blending products formed on the fiber surface [99].

2.4.3. Hollow nanofibers

Hollow nanofibers (Fig. 4a) are considered to be excellent candidates for novel applications, especially in energy storage and sensors. Chemical deposition and coaxial electrospinning techniques are mainly employed to prepare hollow nanofibers [102]. The former technique requires a precursor polymeric nanofiber to be used as a sacrificial template. Targeting materials are coated onto the outer surface of the precursor nanofibers in proper thicknesses. Then, hollow nanofibers can be obtained after removing the templates. For instance, a thin layer of TiO_2 sol was coated on PAN nanofibers (template) to fabricated 135 nm ultrafine TiO_2 hollow nanofibers, which was only about 12.6% of the pristine PAN nanofibers (~1 μm) in size [103].

The process of preparing hollow nanofibers *via* coaxial electrospinning is similar to chemical vapor deposition (CVD) methods. Proper substances are selected as cores and shells separately, and hollow nanofibers are obtained after removing the core materials from the core–shell structures. Compared with the previous method, fabricating hollow nanofibers *via* coaxial electrospinning is more preferred. Since utilizing coaxial electrospinning only concerns the proper post-treatments, which is relatively more straightforward than CVD methods. For instance, $Ce(NO_3)_3$/PVP core–shell nanofibers were prepared *via* coaxial electrospinning method [104]. The core PVP (melting point 130 °C) was easily removed by heating the core–shell nanofibers at a temperature of over 300 °C [104]. Li and Xia fabricated core–shell fibers with PVP/$Ti(O_iPr)_4$ solution and mineral oil. The hollow TiO_2

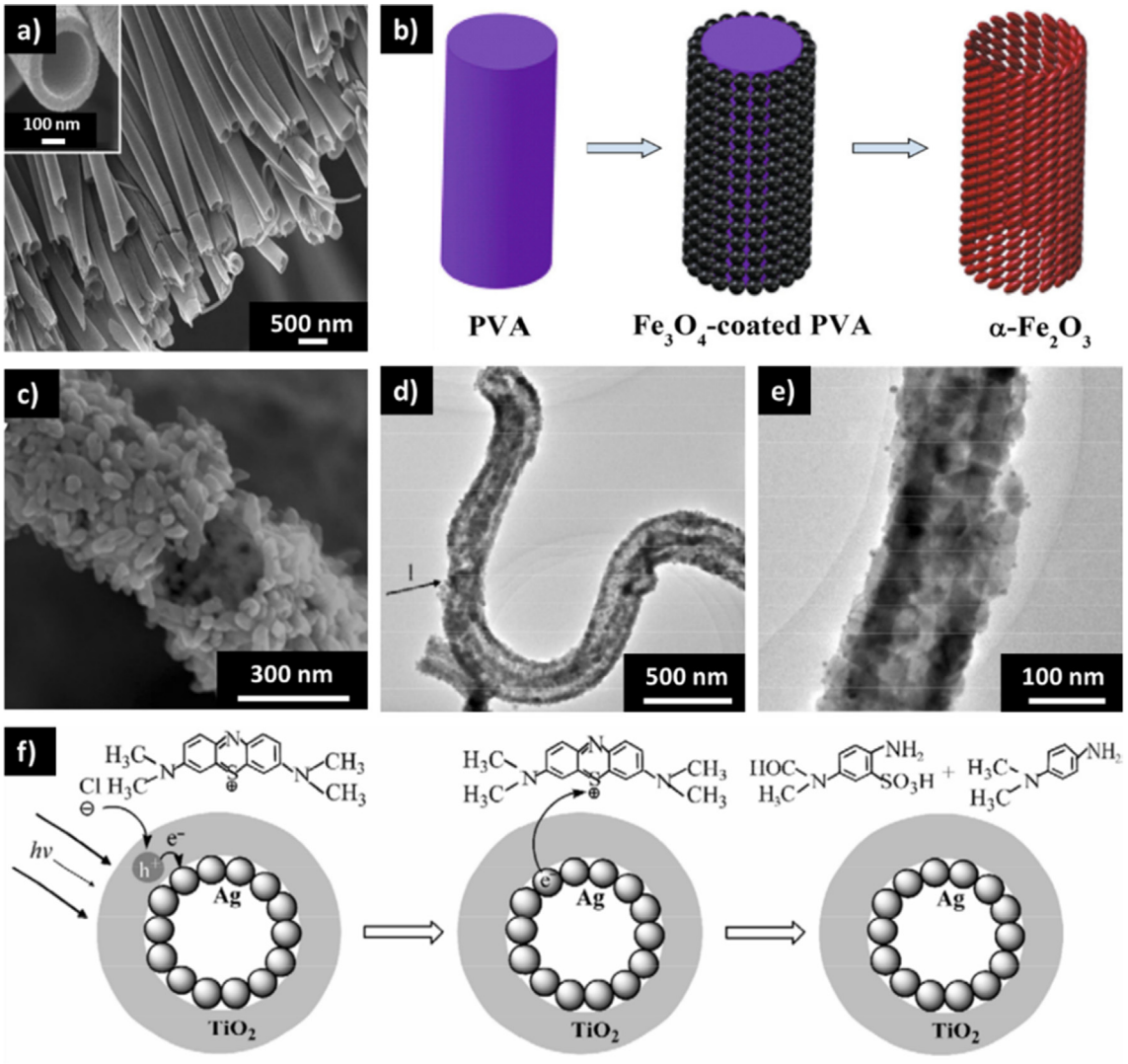

Fig. 4. a) Hollow electrospun nanofibers [105]. Reproduced with permission from [105], Copyright 2004, American Chemical Society. b) Schematic of the preparation process of hollow α-Fe_2O_3 nanofibers [106]. c) FE-SEM image of α-Fe_2O_3 nanofibers prepared *via* 21.1 μmol $FeCl_3{\cdot}6H_2O$/10.5 μmol $FeCl_2{\cdot}4H_2O$/21.2 mol NaOH electrospinning solution [106]. Reproduced with permission from [106], Copyright 2015, Springer Nature. d)-e) TEM and HR-TEM images of Ag nanoparticles filled TiO_2 hollow nanofibers [108]. f) Mechanism of charge injection and separation in Ag nanoparticles filled TiO_2 hollow nanofibers [108]. Reproduced with permission from [108], Copyright 2008, Elsevier. (For interpretation of the references to colour in this figure legend, the reader is referred to the web version of this article.)

nanofibers were obtained after hydrolyzing $Ti(O_iPr)_4$ in the air for 1 h and immersing the nonwovens in octane for overnight [105]. In addition to the simple post-treatment process, manipulating the hollow (core) dimensions *via* changing pinning parameters is relatively easy.

Hollow nanofibers have attracted extensive attention from both academic and industrial communities because of the increased specific surface areas, higher porosity, and permeability, *etc*. Such advantages make the hollow nanofiber into a good purifier, energy capacitor, and sensor, *etc*. For instance, Gao *et al*. tested the absorbability of hollow α-Fe_2O_3 nanofibers with dye [106]. Electrospun PVA nanofiber mat was immersed into degassed $FeCl_3{\cdot}6H_2O/FeCl_2{\cdot}4H_2O$ mixtures for 1 h. The formed PVA-Fe_3O_4 composite was heated at 600 °C to remove the PVA precursor (Fig. 4b). An SEM image of a hollow nanofiber was shown in Fig. 4c. The hollow α-Fe_2O_3 fibers exhibited an absorption capacity of methyl orange (MO) of around 93% in 10 min and 100% in 15 min. This work demonstrated that hollow nanofibers could serve as an excellent adsorbent. Recently, the sensitivity of Pr doped $BiFeO_3$ hollow nanofiber for formaldehyde was tested [107]. Compared with $BiFeO_3$ nanoparticles and $BiFeO_3$ walnut-shaped microspheres, the response rate of hollow $BiFeO_3$ nanofibers to formaldehyde was enhanced by 4.8 and 3.6 times, respectively. Furthermore, the obtained sensors required relatively low operation temperature, which demonstrated the enormous potential of hollow nanofibers being used as a highly sensitive gas sensor. Moreover, the advanced structure of the hollow nanofiber makes it available to cooperate with different materials. For example, Chang *et al*. filled the silver (Ag) nanoparticles into TiO_2 hollow nanofibers *via* coaxial electrospinning. Transmission electron microscopy (TEM) and high-resolution TEM (HR-TEM) images of Ag nanoparticles filled TiO_2 hollow nanofibers were shown in Fig. 4d and 4e. Ag nanoparticles filled in hollow nanofibers were found to possess a better degradation ability other than TiO_2 powders and Ag-TiO_2 fibers. The mechanism of photoactive charge injection and charge separation in Ag nanoparticles was depicted in Fig. 4f [108].

3. Environmental applications of electrospun nanofibers

3.1. Particulate filtration

3.1.1. Mechanism of particulate filtration via fibrous filters

Particulate filtration is a method used to remove PM particles from

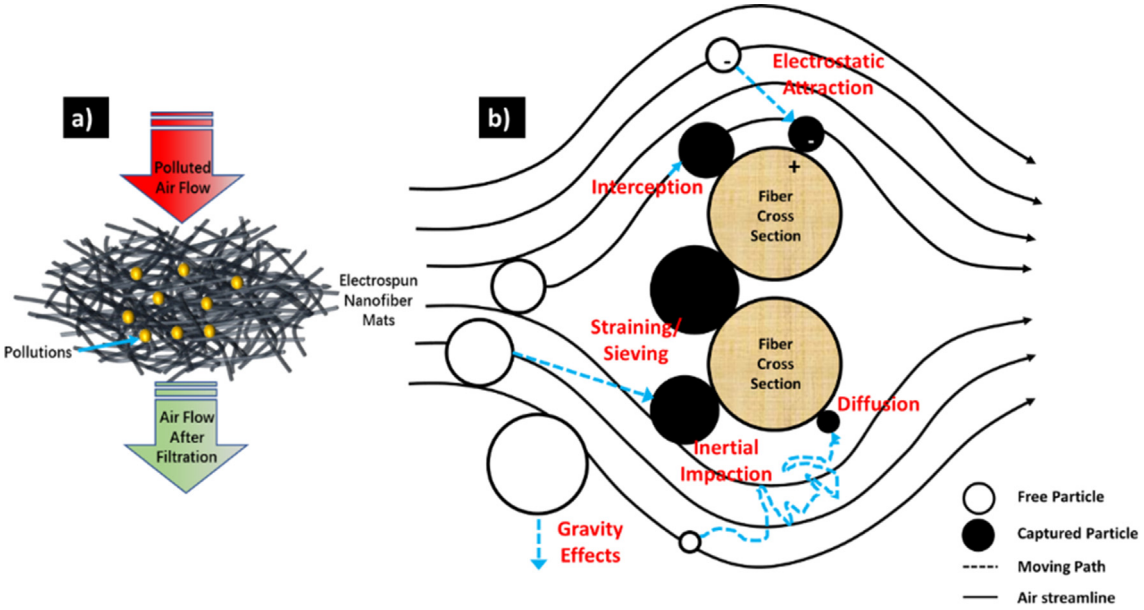

Fig. 5. a) Schematic of polluted air flowing through a fibrous filter. b) Schematic of steady-state filtration mechanism *via* using fibers. (For interpretation of the references to colour in this figure legend, the reader is referred to the web version of this article.)

the air streams (Fig. 5a). As stated, the source and types of particles in the air are different. The mechanisms of particulates removal can be classified into two categories: steady-state and unsteady-state. For the unsteady state, the filter adsorption capacity and pressure drop will change as the filtration process continues. The mechanism of air filtration at the unsteady state is complicated and still underdeveloped. The steady-state mechanism [109,110] of air filtration includes straining, interception, diffusion, inertial impaction, electrostatic effect, and gravity effect (Fig. 5b).

(1) Straining/Sieving. Sieving occurs when the pore size of a membrane is smaller than the sizes of captured particles. A filter works just like a sieve. This effect is closely related to the pore sizes and density of filters.

(2) Inertial impaction. Inertial impaction is based on the sudden change of the airflow direction. Some large particulates (size range 0.3–1 μm) tend to maintain the original moving velocity/path due to the inertia. Therefore, large particles will be separated from the air stream and captured by the filter. The inertial impaction mechanism is applicable when a high concentration of coarse particles exists.

(3) Interception. Interception involves physical contact between particles and fibers. As particles transfer through the fibrous matrix, they will move closely to fibers and be captured by van der Waals forces. The intercepted particles are smaller than the particles captured by the inertia impaction. It should be noted that sieving, inertia impaction, and interception are dominant filtration mechanisms for the particle size larger than 0.2 μm.

(4) Diffusion. The diffusion mechanism is applicable for gas molecules and small particles (sizes range smaller than 0.2 μm). Small particles and molecules collide with each other and move in random directions. Such phenomena are widely known as Brownian motion. Thus, the more intensive the random movement, the more likely the fibers are to catch small particles. Diffusion mainly occurs when air stream passes through a filter in low velocities.

(5) Electrostatic attraction. Electrostatic attraction involves the charged particles and charged fibrous collectors. Fibers attract particles if they are oppositely charged. Otherwise, particles will be repelled by the filters with the same charges. Electrostatic attraction is utilized for removing fine particulates, such as PM 2.5 (the dynamic diameters of PM particles are smaller than 2.5 μm) and smoke.

(6) Gravity effects. Gravity effect means particulates will precipitate due to the gravitational force. This mechanism is only applicable when the particle size is larger than 0.5 μm.

3.1.2. The advantages of electrospun nanofibrous particulate filters

The conventional particulate filters include fabrics, porous ceramics, glass fibers, papers, and active carbon, *etc*. A fabric filter is considered as a stable, economical material to remove particles in the airflow. The fabric filters are efficient on the removal of particles with sizes in microscale and larger than filter openings. As the airflow passes through a fabric filter, the particles will be intercepted on the fabric surface. Only when a certain thickness of dust is built on the surface, will the fabric filters be effective for the removal of fine particulates. Once the particulate layer is damaged or removed, the filtration efficiency of fabric filters will be tremendously reduced. Therefore, the current fabric filters cannot fully satisfy the rising standards of living qualities due to rapidly worsening PM pollutions.

The filter performance is highly affected by fiber sizes [111,112], specific surface areas [113], mat base weight [114], and packing densities [115], *etc*. Since the 1980s, electrospun nanofibers have been used as particle filters to remove air pollutants [116]. Electrospun nanofibrous membranes have advantages such as higher porosity (80–90%), smaller fiber size (nanoscale), and larger specific surface area, which are considered to be valid promotions compared with the microscale filters. Therefore, electrospun nanofibers have shown a promising future of being used as high-efficiency air filtration media.

3.1.3. Performance evaluations

In most cases, the filtration process is strongly related to air pressure drop, airflow velocities, and filtration areas, *etc*. The proper filter selection is usually characterized by filtration efficiency and airflow resistance.

The particle collecting efficiency refers to the ability of filter capturing dusts or pollutions and is evaluated as [110]

$$\eta = \left(1 - \frac{C_2}{C_1}\right) \times 100\% \quad (1)$$

where η is the collection efficiency, C_1 and C_2 represent the concentrations of contaminants in the airflow before and after filtration, respectively.

Air filter inevitably forms resistance to the airflow passing through,

and filtration resistance continues adding as the filter keeps collecting dusts. When the resistance increases to a certain value, the filter will be scrapped and should be replaced. Thus, the final resistance of the filter Rf is directly linked to the service life of the filter, and the selection and design of the filter must be determined at a given airflow velocity. This parameter can be evaluated by the following equation [110]

$$R_f = \frac{\Delta P}{v} \tag{2}$$

where ΔP is the pressure drop, and v is the air velocity passing through the filter.

The quality factor (QF) needs to be considered for the filtration performance evaluations. Larger value of QF indicates a better filtration performance. The corresponding formula of QF reads [110]

$$QF = -\frac{ln(1-\eta)}{\Delta P} \tag{3}$$

3.1.4. Electrospun particulate filters

3.1.4.1. Single-component nanofibrous particulate filters. Nanofibrous filters prepared *via* synthetic polymers have the advantages of high mechanical properties and high filtration efficiency. Kim *et al.* investigated the filtration performance of a uniform nylon-6 nanofibrous filter for 0.02–1.0 μm particles. This filter was electrospun *via* nylon-6 and formic acid (FA) solution. The filtration efficiency of this single-component filter was measured as 99.98% (264.8 Pa pressure drop) [117]. Similarly, Matulevicius *et al.* obtained 535 nm diameter of PAN nanofiber mats and demonstrated that this uniform filter could remove 100 nm and 300 nm polystyrene latex (PSL) particles with 98.01% and 95.83% filtration efficiency (90.37 Pa pressure drop), respectively [118]. Meanwhile, Matulevicius *et al.* reported that 399 nm diameter of polyvinyl acetate (PVAc) nanofibers, which processed beaded structure (Fig. 6a), exhibited 99.57% and 97.38% filtration efficiency for 100 nm and 300 nm PSL particles (132.83 Pa pressure drop), respectively [118]. Xu *et al.* reported the filtration performance of transparent nylon-6 electrospun nanofibers [119]. The removal efficiency for PM 2.5 was measured as 99.56% (270 Pa pressure drop), and the quality factor was calculated as 0.020. This filter performed much better than the commercial high-efficiency air filters. SEM images of PI nanofibers before and after filtration were shown in Fig. 6b and 6e. Furthermore, they developed a faster and larger-scale film transferring method, which could realize the roll-to-roll production of transparent membranes and be beneficial for further commercialization of the electrospinning process (Fig. 6c) [119].

Currently, natural polymers like chitosan and cellulose have attracted great interests due to their green, renewable, and degradable properties. However, some natural polymers are sensitive to the working temperature and the surrounding pH value. High working temperature may decrease the solution viscosity and diameters of nanofibers [71–73]. In some of electrospinning processes, increasing surrounding temperature by heaters to reduce the working humidity are required [17,18]. However, the changes of working temperature can affect mechanical properties of naturally polymeric nanofibers and reduce their applicability of being used as high-performance particulate filters. The changes in pH value can cause partial ionization and greatly affect activities of some natural polymers [120]. Meanwhile, pH value may influence the viscosity of prepared polymeric solution and result in the undesirable fiber morphologies. Therefore, attention should be drawn when preparing naturally polymeric solutions in electrospinning process. A mixture contained 62 wt% acetone, 31 wt% dimethyl sulfoxide, and 7 wt% acetic acid (AA) was prepared to dissolve CA in the work of Nicosia et al. [121]. They controlled the operating temperature and the pH value of solvent to form a stable CA suspension. These components also ensured that CA nanofibers process beads-free structure and leave no residues in the final CA nanofibers. Fabricated samples could remove only 80% particles (diameter larger than 0.4 μm) in the air streams [121]. Thus, utilizing natural polymers as particulate filters are limited comparing with synthetic polymers.

3.1.4.2. Multi-component nanofibrous particulate filters. Compared with single-component nanofibers discussed above, adding additives to electrospinning solutions or combining synthetic and natural polymers can change the solution properties and improve the filtration performance of electrospun filters.

First, adding metal oxides to synthetically polymeric solutions can decrease the solution viscosity and conductivity, and increase the fiber surface roughness by introducing nanoscale protrusions. Commonly used metal oxides are titanium dioxide (TiO_2), silicon dioxide (SiO_2), and aluminum oxide (Al_2O_3). Cho *et al.* measured the filtration efficiency of PAN/TiO_2 hybrid nanofibers for PM particles. SEM images of PAN/TiO_2 hybrid nanofibers before and after the filtration process were shown in Fig. 7a and 7b. These nanofibers were prepared *via* mixing 5–10 nm TiO_2 nanoparticles into PAN/DMF solutions. Compared with pristine PAN nanofibers, the average diameter of hybrid nanofibers was found to be slightly reduced, and the corresponding filtration efficiency was 4–6% higher than pure PAN nanofibers [49]. Yu *et al.* fabricated flexible PAN composite nanofiber with SiO_2 aerogel [122]. Compared with pure PAN membrane, SiO_2 aerogels could increase the filtration capacity of the hybrid PAN membrane by over 2.5 times. Moreover,

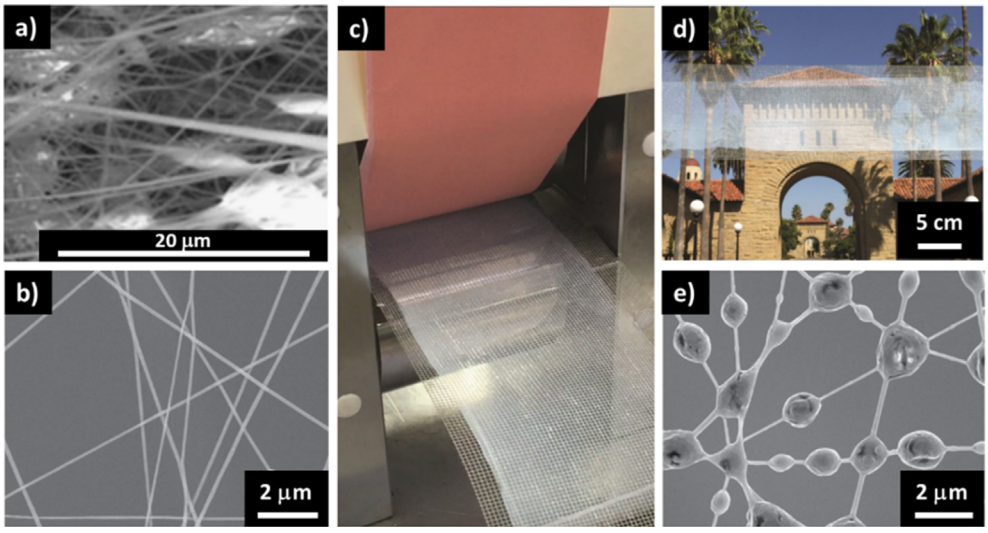

Fig. 6. a) Beaded PVAc nanofibers [118]. Reproduced with permission from [118], Copyright 2016, Elsevier. b) Nylon-6 electrospun nanofibers before filtration process [119]. c) Image of roll-to-roll production of transparent PM filter [119]. d) Transparent PM filter produced through the developed roll-to-roll production method [119]. e) Nylon-6 electrospun nanofibers after filtration process [119]. Reproduced with permission from [119], Copyright 2016, American Chemical Society. (For interpretation of the references to colour in this figure legend, the reader is referred to the web version of this article.)

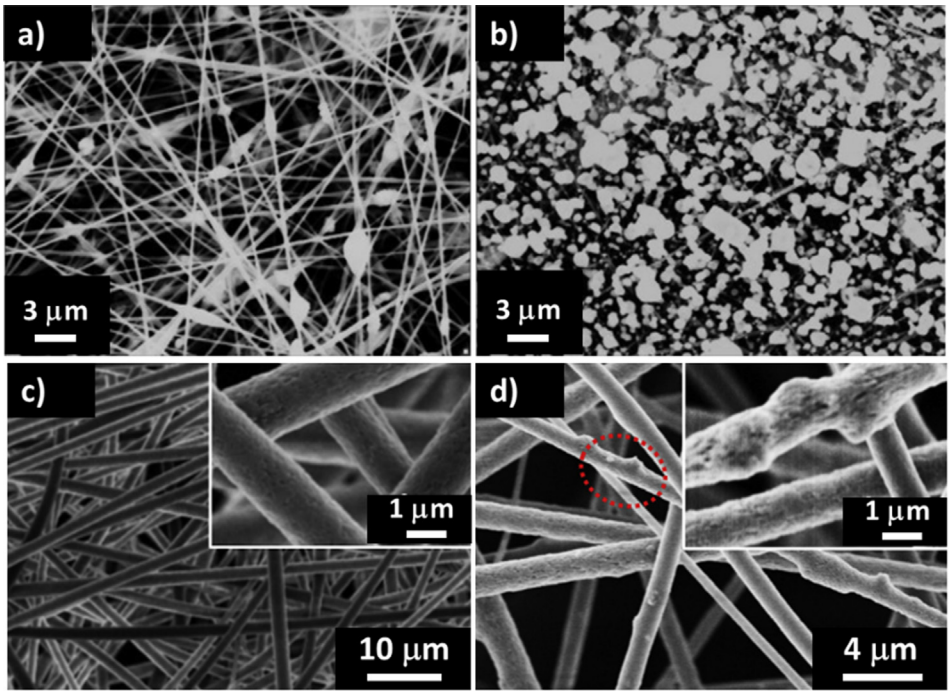

Fig. 7. a)-b) 0.5 g/ft^2 PAN/TiO_2 fibers before and after filtration process [49]. Reproduced with permission from [49], Copyright 2013, Elsevier. c) FE-SEM image of smoothly structured PSU electrospun nanofibers [123]. d) FE-SEM image of hierarchically structured PSU/7.5 wt% TiO_2 electrospun nanofibers [123]. Reproduced with permission from [123], Copyright 2014, Elsevier. (For interpretation of the references to colour in this figure legend, the reader is referred to the web version of this article.)

adding metal oxides can make nanofibers gain extra functionalities. Wan *et al.* developed air filtration media with polysulfone (PSU)/TiO_2 nanofibers [123]. Hierarchical nanostructure, which was introduced by the added nanoparticles, resulted in the superhydrophobic properties. Morphological comparisons of intrinsic PSU and PSU/TiO_2 hybrid nanofibers were shown in Fig. 7c and 7d. The filtration efficiency of this multi-component filter was booted up to 99.997% (45.3 Pa pressure drop), and a promising superhydrophobicity (the water contact angle (WCA) up to 152°) was exhibited [123].

On the other hand, the combination of natural and synthetic polymers can decrease fiber size, enhance mechanical properties, and improve the filtration performance (not only limited to particulate removal) of electrospun nanofibers. For instance, cyclodextrins (CD) was added to enhance the viscosity and conductivity of the low concentration polyethylene terephthalate (PET) solutions and led to the beads-free PET/CD nanofibers [124]. In this case, the aniline vapor filtration performance of intrinsic PET nanofibers was enhanced by about 1.8 times through adding CD in the mixture [124]. In another case, poly (methyl methacrylate) (PMMA) nanofibers with 10% β-CD were capable of trapping styrene molecules after 3 h exposure in the vapor, while pure PMMA electrospun nano-webs did not show any capturing capabilities. The capturing performance increased as the increasing amounts of β-CD contained in PMMA nano-webs [125]. Moreover, chitosan and PEO dissolved in AA together in the ratio of 9:1 were utilized to make beadless nanofibers. The fiber diameter and maximum pore size were measured as 92 nm and 1.562 μm, respectively. In this case, a 1 GSM (gram per square meter) beads-free chitosan/PEO nanofiber sample could achieve ~50% filtration efficiency of removing 200 ppm PS particles in airflow, and ~70% filtration efficiency was exhibited by 3 GSM sample [50].

It should be noticed that the working temperature of polymeric media such as PAN and nylon-6 was lower than 150 °C. Since single-component filters that were made from such polymers could not sustain their filtration performance at high temperature and fulfill the severely industrial requirements. Zhang *et al.* developed high-temperature resistant PI nanofiber mats that could be used as an air filter for PM2.5 at high temperature. The filtration efficiency of this PI filter was measured as 99.5%, and the corresponding filtration performance was still maintained at 370 °C [57]. Optical microscopy (OM) and SEM images of this PI air filter after the filtration process were shown in Fig. 8a and 8b, repectively. PM particles were found to be caught as soon as they got in touch with fibrous matrices. The capturing process was studied by the experimental apparatus shown in Fig. 8c. During the experiments, solid particulates were captured by fibers or attracted by those captured particles. Eventually, large numbers of dendrite-like structures were formed (Fig. 8d and 8e). In this work, the filtration processes of water droplets and oil droplets generated by cigarette smoke were also studied. Different from coalescent behavior of liquid droplets, the captured particles were noticed to be separable by the strong gas flow [126]. This phenomenon was caused by the weak adhesion of particultes with nanofibers and would result in the reduction of filtration efficiency.

3.2. Heavy metal ion adsorptions

3.2.1. Common heavy metal ions found in the environment

Heavy metal refers to metal and metalloid elements whose density ranging from 3.5 to 7 g/cm^3 [127]. Currently, heavy metal elements found in the hydrological system include mercury (Hg), copper (Cu), cadmium (Cd), chromium (Cr), thallium (Tl), zinc (Zn), nickel (Ni), and lead (Pb), *etc*. The release of heavy metal ions into natural environments comes from two sources, natural process and anthropogenic activities. Natural discharging sources of heavy metal include volcanic activity, forest fire, and seepage in rocks, *etc*. Most anthropogenic disregards that contain high concentrations of heavy metals come from industrial activities, such as electroplating and batteries [128]. Regular amounts of organic pollutions can be biodegraded, while the heavy metal contaminants are not consumable by the natural system and will progressively be accumulated by the living organisms. A few heavy metal ions are essential supplements for the human body's health. However, excess doses will be poisonous and lethal. Therefore, it is necessary to pre-treat the contaminated wastewater before it is discharged into the environment.

3.2.2. Conventional heavy metal absorbents and mechanisms

Traditional heavy metal removal methods include chemical precipitation, solvent extraction, membrane filtration, ion exchange, electrochemical removal, coagulation, flotation, irradiation, and ozonation [129], *etc*. However, these treatment processes have many

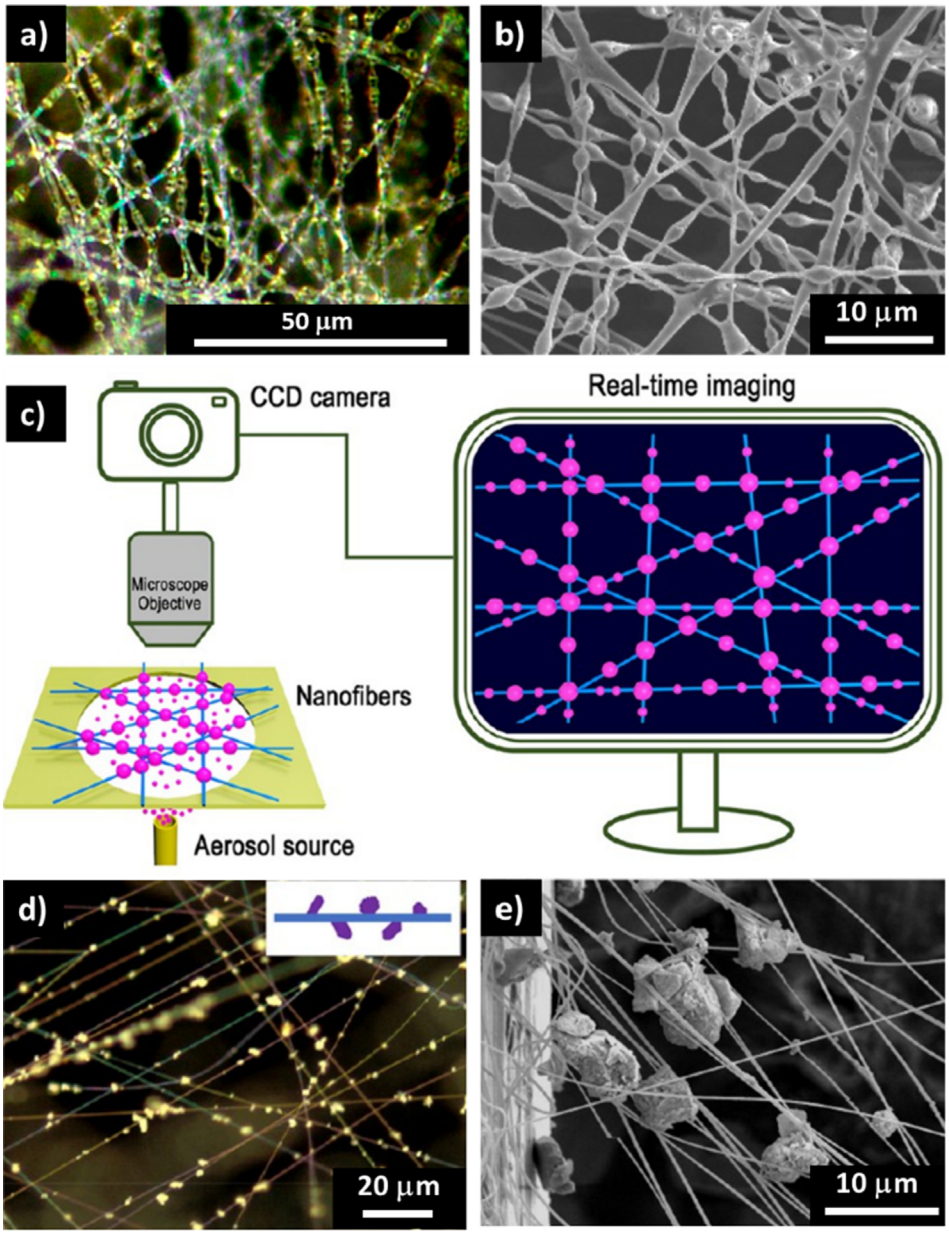

Fig. 8. a)-b) OM and SEM images of a high-temperature resistant PI air filter after the filtration process [57]. Reproduced with permission from [57], Copyright 2016, American Chemical Society. c) Schematic of the experimental setup of the *in situ* investigation on the particle removal [126]. d) Image of solid particulates on nanofibers [126]. e) SEM image of captured particulates [126]. Reproduced with permission from [126], Copyright 2018, American Chemical Society. (For interpretation of the references to colour in this figure legend, the reader is referred to the web version of this article.)

disadvantages. For instance, chemical precipitation process requires a vast amount of chemicals to remove metal ions and post-treatments to adjust pH value of discharges. The solvent extraction method consumes a considerable amount of energy and requires highly selective extractant, which tremendously increases the handling cost.

In recent years, numerous studies have focused on the development of more effective and economical removal techniques. Adsorption is considered as an alternative method. Since absorbents are relatively cheap, and the adsorption process will not generate secondary pollutants. Adsorption processes can be classified into physisorption (physical adsorption) and chemisorption (chemical adsorption). During the physical adsorption process, molecules transferring through the porous media will be physically adsorbed by the porous skeleton due to the van der Waals forces, and the adsorbed molecules will be desorbed at the same time. Physisorption progress is highly dependent on the surrounding temperature and pressure. Chemisorption involves electron transfer between adsorbents and adsorbates [130]. In the process of chemisorption, including covalent bond and ionic bond, strong interaction occurs. The chemical adsorption, which is usually irreversible and highly selective, require certain energy for activation. Both chemisorption and physisorption performance are proportional to the surface area of absorbents.

Several substances can be used as heavy metal absorbents. Zeolites, active carbons, bentonite, metal oxides are conventional absorbents. For example, active carbons are widely applied as absorbents due to their large specific areas and excellent absorption capacities [131–133]. Zeolites process excellent ion exchange properties since it is composed of hydrated aluminosilicate minerals [134]. However, conventional absorbents are limited by the disadvantages of high production cost, low reusability, and low selectivity for the targeting absorbates. Although some of adsorbents can be treated to be reusable, the processing progress is not very eco-friendly and may cause economic loss. Thus,

alternative absorbents are still highly requested.

3.2.3. Electrospun nanofibers used as adsorbents for heavy metal ions

The nanofibrous membrane has attracted significant attention due to its high porosity, large specific surface area, and high liquid permeability. The performance of nanofibrous filters is affected by solution pH values, contact time of ions with absorbents, solution temperature, and initial concentration of metal ions. In this subsection, we summarized some functional fibers used as absorbents for the removal of heavy metal ions [135].

3.2.3.1. Single-component absorbents for heavy metal removal. Single-component nanofibers are fabricated for the removal of heavy metal ions removal from wastewater. Some polymeric nanofibers do not exhibit any capabilities in adsorbing heavy metal ions. For instance, PAN nanofibers exhibit superior mechanical properties and filtration performance in air filtration. However, pristine PAN nano-membranes are not capable of removing heavy metal ions in wastewater [136]. In contrary, some pristine polymeric nanofibers do exhibit the heavy metal absorbability. In one case, the PVA electrospun fiber mat was placed in pH 5–6 solutions for 60 min to remove Cu (II) ions, and the adsorption capacity was obtained as 124.34 mg/g [137]. Haider and Park reported that the equilibrium adsorption capacity of chitosan nanofibers for Cu (II) and Pb (II) were 485.44 and 263.15 mg/g, respectively, after placing in the 400 ppm model solutions for 24 h [138]. However, the removal performance of some pristine electrospun nanofibers is not comparable to the modified membranes. Thus, single-component electrospun nanofibers are not very good options to be employed directly to remove the heavy metal ions.

3.2.3.2. Modified heavy metal ions absorbents. Modifications to well-fabricated electrospun nanofibers can be realized *via* chemical reactions or post-coatings. The membrane modifications aim at enhancing the heavy metal removal performance of nanofibers from the polluted water, increasing the fiber adaptabilities to maintain the performance under different testing conditions, enhancing the membrane selectivity, and improving the fibrous membrane reusability. So far, there are two methods considered as effective modification methods, grafting functional groups to electrospun nanofibers and developing nanofibers with unique functions.

Grafting functional groups (like -COOH, -SH, and -NH_2) to polymeric materials is an effective method to improve the performance of absorbents [39]. The functional groups in the added components can promote the reactions between primary groups in polymers and heavy metal ions, thus improving the removal efficiency. For instance, the -OH group in cellulose could facilitate the chelation of heavy metal ions with -NH_2 and -OH groups in chitosan. Choi *et al.* reported a larger surface area of titanium–zirconium oxide nanofibrous mat through inducing the phosphonate and amine groups to nanofibers [139]. The specific surface area was enhanced to 248 m^2/g, and the cadmium adsorption capacity was tremendously increased comparing with the non-modified nanofibers [139]. Stephen *et al.* prepared the electrospinning solutions with 16% CA dissolved in acetone/N, N-dimethylacetamide mixtures [140]. The fabricated nonwovens were immersed in oxolane-2,5-dione mixtures to functionalize cellulose-g-oxolane-2,5-dione (Fig. 9a and 9b). Such modifications resulted in 384.86 nm diameter of nanofibers and 13.68 m^2/g specific surface area of the membrane. The maximum adsorption capacity of Cd (II) and Pb (II) ions were obtained as 2.91 and 1.0 mmol/g, respectively. The modified cellulose nanofibers possessed excellent reusability and similar adsorption capacities with commercial products [140]. Feng *et al.* obtained amidoxime polyacrylonitrile/regenerate cellulose (AOPAN/RC) nanofiber membrane by immersing PAN/CA electrospun nanofiber in NaOH solutions for 24 h and then hydroxylamine hydrochloride/Na_2CO_3 for an additional 2 h. The schematic of the synthesis process was shown in Fig. 9c. Such modification converted -C≡N group into -C(NH_2) = NOH group, which tremendously enhanced the capacities of heavy metal removal. Fe (III), Cu (II), and Cd (II) maximum adsorption capacity of AOPAN/RC nanofibers was detected as 7.47, 4.26, and 1.13 mmol/g, respectively (Fig. 9d) [141]. Moreover, the modified thiol-functionalized cellulose nanofibers were produced *via* esterification reaction with DTDPA (3,3-dithiodipropionic acid) by CDI (1,1-carbonyldiimidazole) coupling and 3 h immersion in AmTG (ammonium thioglycolate) aqueous solutions (Fig. 9e). The maximum adsorption capacity of Cu (II), Cd (II), and Pb (II) ions at pH = 4 were obtained as 49.0, 45.9, and 22.0 mg/g, respectively [59].

In addition to the above methods, specialized functional nanofibers also contribute to heavy metal removal. Introducing functionalized metal oxide compounds to nanofibers can fabricated magnetic fibers. Zhao *et al.* produced magnetic iron oxide/polyacrylonitrile electrospun (b-PEI-FePAN) fibers (Fig. 10a). The maximum Cr (VI) adsorption capacity of prepared magnetic electrospun fibers was measured as 684.93 mg/g [58]. SEM images of b-PEI-FePAN fibers were shown in Fig. 10b and 10c, respectively. Shi *et al.* prepared the magnetic fibers by the novel sol–gel method [142]. The synthesis process of the sol–gel method was shown in Fig. 10d. The BET surface area of fiber mats was obtained as 51.03 m^2/g, and the Pb (II) adsorption capacities at room temperature were measured as 16.78 mg/g [142]. SEM images of Fe_3O_4 electrospun fibers were shown in Fig. 10e and 10f. These novel approaches have attracted much attention due to their advantages of non-agglomeration of absorbates and easy separation of absorbents. Such developments can contribute to the reusability enhancement of the nonwoven mats. Furthermore, Bornillo *et al.* reported that the stimuli-responsive polymers also could be used as an alternative way to enhance the adsorption efficiency since this polymer could self-adjust based on the environment. This work used dual-responsive polyethersulfone-poly (dimethyl amino) ethyl methacrylate (PES-PDMAEMA) nanofiber mats as adsorbents. The maximum adsorption amount of Cu (II) obtained at pH 6.5 at 55 °C and the corresponding quantity was 161.3 mg/g [143]. This filtration material had strong adaptability. Therefore, it can be used under severe working conditions and has extended serving life.

3.3. Self-cleaning electrospun nanofibers

Some applications are sensitive to their surface contamination. For instance, water vapors deposited on the protective glass will block the view. Particulate matters suspended in the atmosphere will inevitably pollute solar panels and reduce the output power. The regular maintain process of these applications is either expensive or not timely. Thus, further cost-effective developments are high requested.

3.3.1. Brief introduction of self-cleaning surface

Dust, pollutants, or bacteria attached to the self-cleaning surface can be degraded or removed only *via* natural aids, including gravity, raindrops, and sunlight, *etc*. These functionalities can sustain the surface clean and save maintenance costs. The self-cleaning surface can be classified into two categories based on its wettability: hydrophobic and hydrophilic. The contact angle and sliding angle of a water droplet on the surface characterize the surface ability to cleanness. On the hydrophobic surface, WCA will be larger than 90° (larger than 150° will be considered as superhydrophobic), and the sliding angle is less than 10° [144]. Larger WCA indicates a better surface hydrophobicity. WCA on the hydrophilic surface will be smaller than 10° (less than 5° will be considered as superhydrophilic) [145].

The self-cleaning hydrophobic property was inspired by the surface features of lotus leaves, *i.e.*, the lotus effect (Fig. 11a). The hierarchical structures of lotus surfaces, which are formed by the characteristic epidermis and the covering wax, are responsible for the lotus self-cleaning property (Fig. 11b and 11c). Such microscale structures result in spherical water droplets and minimize the adhesion energies and contact areas of water droplets to the leaf surfaces [146]. Thus, dirt

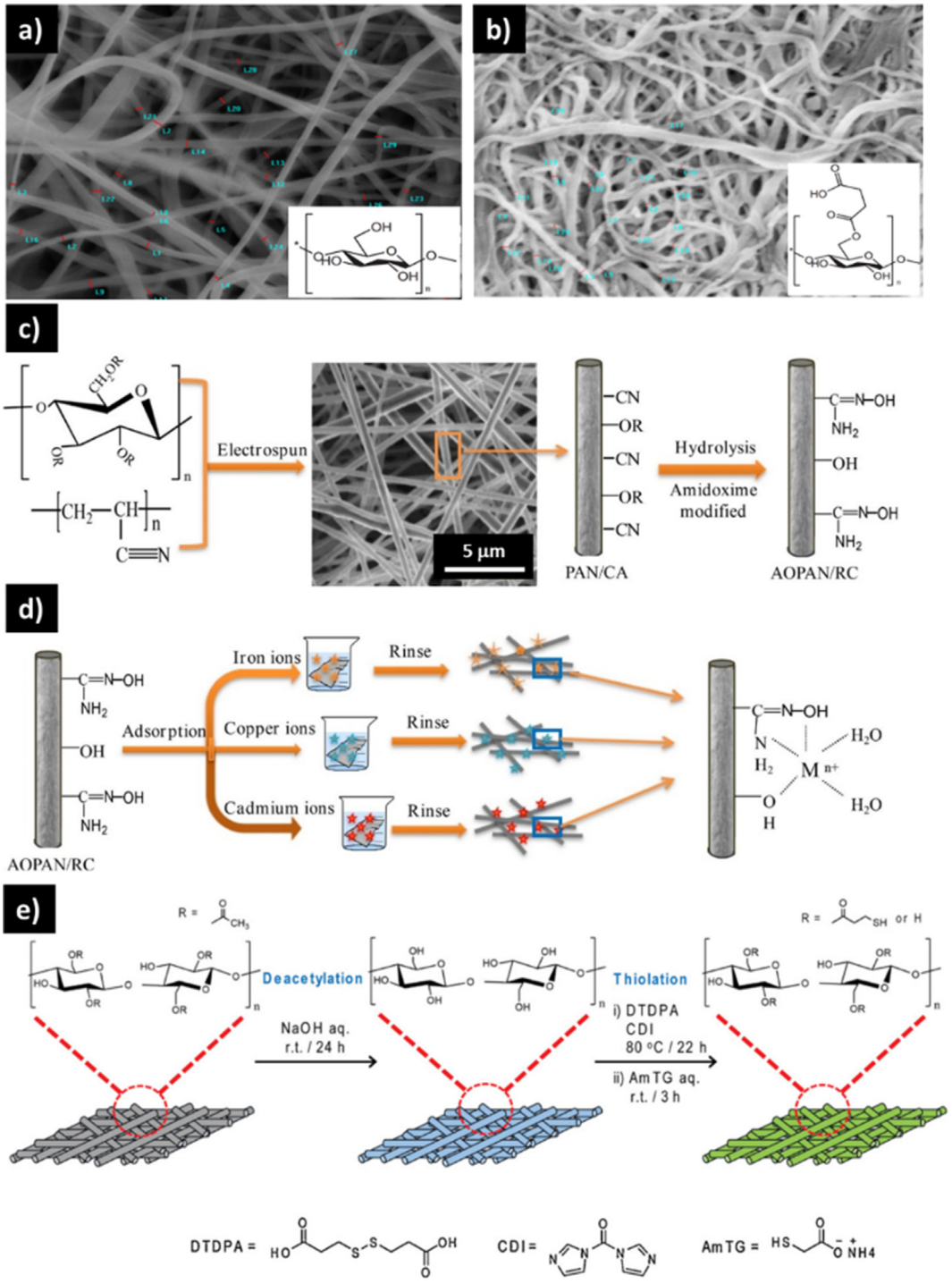

Fig. 9. a)-b) SEM images of cellulose nanofibers and cellulose-g-oxolane-2,5-dione nanofibers [140]. Reproduced with permission from [140], Copyright 2011, Elsevier. c) Schematic of the preparation process for AOPAN/RC nanofibers [141]. d) Schematic of the heavy metal removal process by using AOPAN/RC nanofibers [141]. Reproduced with permission from [141], Copyright 2018, Elsevier. e) Schematic of the fabrication process for thiol-functionalized cellulose nanofibers [59]. Reproduced with permission from [59], Copyright 2020, Elsevier. (For interpretation of the references to colour in this figure legend, the reader is referred to the web version of this article.)

particles on the lotus leaves can be easily picked up and removed with rolling water droplets (Fig. 11d).

On the contrary, water in contact with self-cleaning hydrophilic surface will spread rapidly with a minimal contact angle, forming a uniform membrane. This water film will spread beneath the dirt particles and make contaminates loose. The contaminates will be washed away when the water film is running off (Fig. 12a). Self-cleaning hydrophilic surface using metal oxides can degrade or decompose the organic pollutants. Such self-purification functionalities are realized by adding photocatalyst to the targeting surface. Sunlight is required to activate this chemical reaction process [148]. Here we take TiO_2, the most common photocatalyst, as an example to briefly introduce the photocatalytic oxidation mechanism. First, the catalyst electrons will stay in the valance band if the energy of light irradiation is lower than the bandgap of the photocatalyst. Then, electrons (e^-) will move to the conduction band if higher energy is provided and leave the holes (h^+)

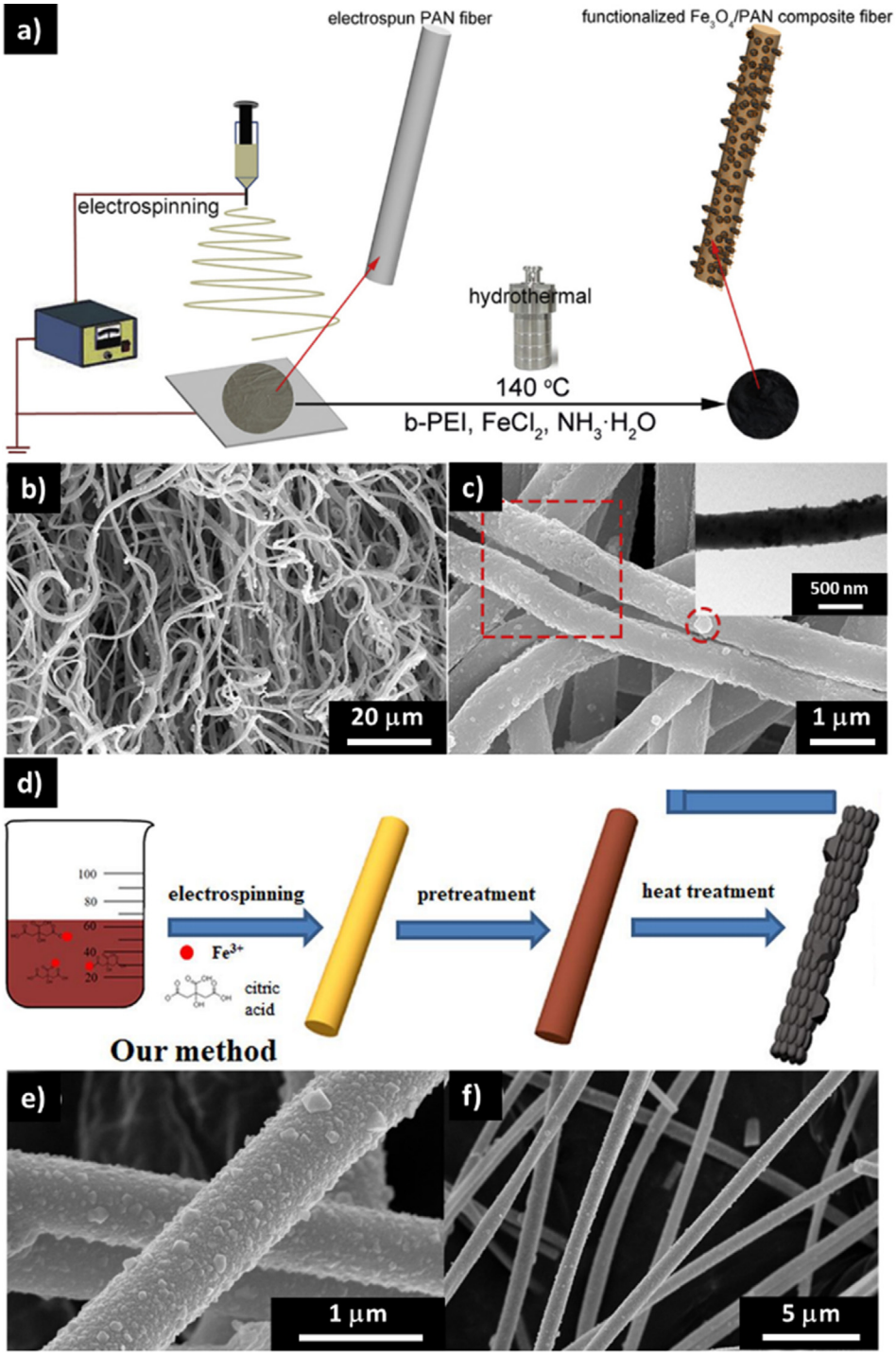

Fig. 10. a) Schematic of the synthesis process for Fe_3O_4/PAN electrospun fibers [58]. b)-c) SEM images of b-PEI-FePAN fibers [58]. Reproduced with permission from [58], Copyright 2017, Elsevier. d) Schematic of the preparation process for flexible Fe_3O_4 electrospun fibers [142]. e)-f) SEM images of Fe_3O_4 electrospun fibers [142]. Reproduced with permission from [142], Copyright 2020, Elsevier. (For interpretation of the references to colour in this figure legend, the reader is referred to the web version of this article.)

in the valance band. Generated electrons (e^-) and holes (h^+) may be consumed in three possible ways: (i) electrons (e^-) and holes (h^+) recombine with each other and release heat; (ii) electrons (e^-) diffuse to the catalyst surface and initiate the redox reactions with the pollutants; (iii) holes (h^+) react with water or hydroxide ions to generate hydroxyl radicals (-OH), which contain tremendous power to oxide the contaminates and decompose the attached pollutions [149–152]. The schematic of the stated photocatalytic oxidation mechanism was drawn in Fig. 12b and 12c, respectively.

The industrial and academic communities have shown great enthusiasm for self-cleaning techniques, especially the development of the self-cleaning hydrophobic surface. In recent years, many technologies have been developed to prepare the self-cleaning hydrophobic surface, such as dip-coating technique [153,154], spray coating [155,156], spin coating [153], and electrospray/electrospinning coating method [157]. Currently, the practical applications of self-cleaning surfaces include anti-fogging, anti-corrosion, UV protection clothing, photovoltaic devices, and anti-reflective coating, *etc*. However, difficulties always exist

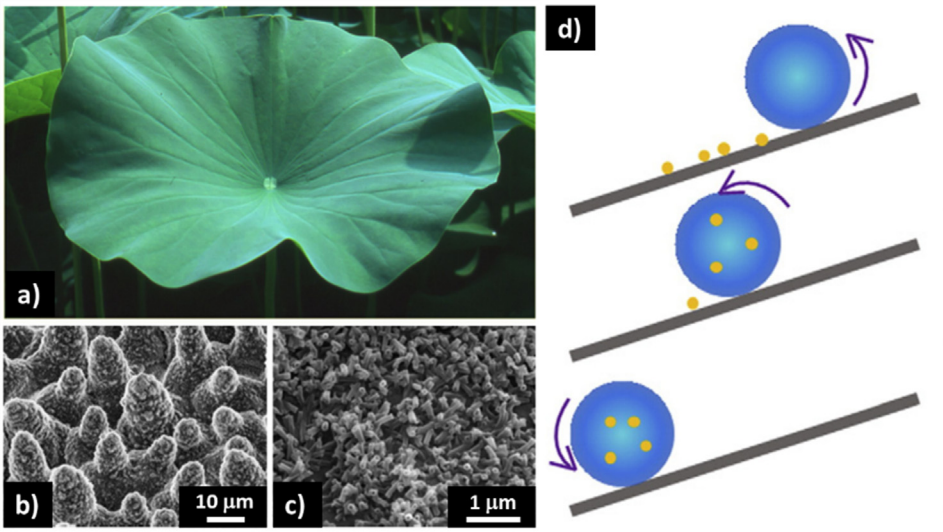

Fig. 11. (a) The lotus leaves [146]. (b) SEM image of the upper lotus leaf side [146]. (c) Wax tubules on the upper lotus leaf side [146]. Reproduced with permission from [146], Copyright 2011, Beilstein-Institut. d) Schematic of rolling water droplet washes out particulates on the surface with high contact angle [147]. Reproduced with permission from [147], Copyright 2016, Elsevier. (For interpretation of the references to colour in this figure legend, the reader is referred to the web version of this article.)

in the developing process of self-cleaning surfaces. Improving the durability and stability under harsh environmental conditions are the biggest challenges for hydrophobic surface fabrication [158], while enhancing the utilization rate of the UV portion of the sunlight with less complexity and costs are the most significant practical problem for the development of self-cleaning hydrophilic surfaces [148].

3.3.2. Self-cleaning hydrophobic electrospun nanofibers

Self-cleaning hydrophobic surfaces require large surface roughness and low surface free energy. Electrospun nanofibers have advantages to satisfy the above-mentioned requirements. Several approaches were made for the development of the self-cleaning hydrophobic electrospun nanofibers, (i) utilizing hydrophobic materials, (ii) biomimeticing hydrophobic structure, and (iii) post-treating electrospun nanofibers.

3.3.2.1. Self-cleaning hydrophobic nanofibers via utilizing hydrophobic substance. Hydrophobic nanofibers are successfully fabricated *via* single-component electrospinning solutions. The conventional hydrophobic polymers include PS, PCL, and polyethylene (PE), *etc*. Lee *et al*. prepared smooth PS nanofibers *via* electrospinning method and applied the obtained membrane for the oil–water separation experiments. The pristine PS nanofibers inherited the water-repellency from PS material. The contact angle of a water droplet on the PS nanofiber surface was 155°, which indicated its good hydrophobicity [159]. In another case, 17 wt% PCL dissolved in DMF/methylene chloride (MC) solvent was used as the electrospinning materials. The obtained fiber size in the range of 400 nm ~ 1.6 μm. The water contact angle was around 128.5°[160]. In the same work, 1 wt% PCL in DMF/MC solution was fabricated through the electrostatic process and resulted in the nanofiber-droplets

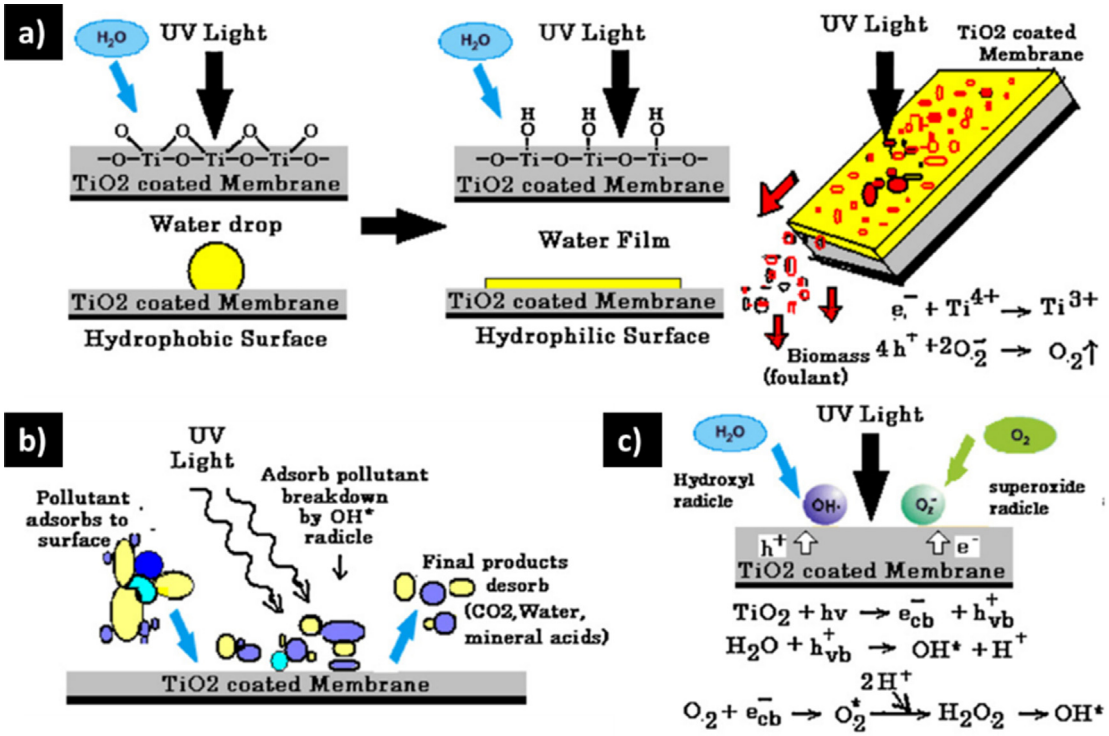

Fig. 12. a) Schematic of the self-cleaning hydrophilic surface [152]. b)-c) Schematic of the photocatalytic oxidation mechanism [152]. Reproduced with permission from [152], Copyright 2009, Elsevier. (For interpretation of the references to colour in this figure legend, the reader is referred to the web version of this article.)

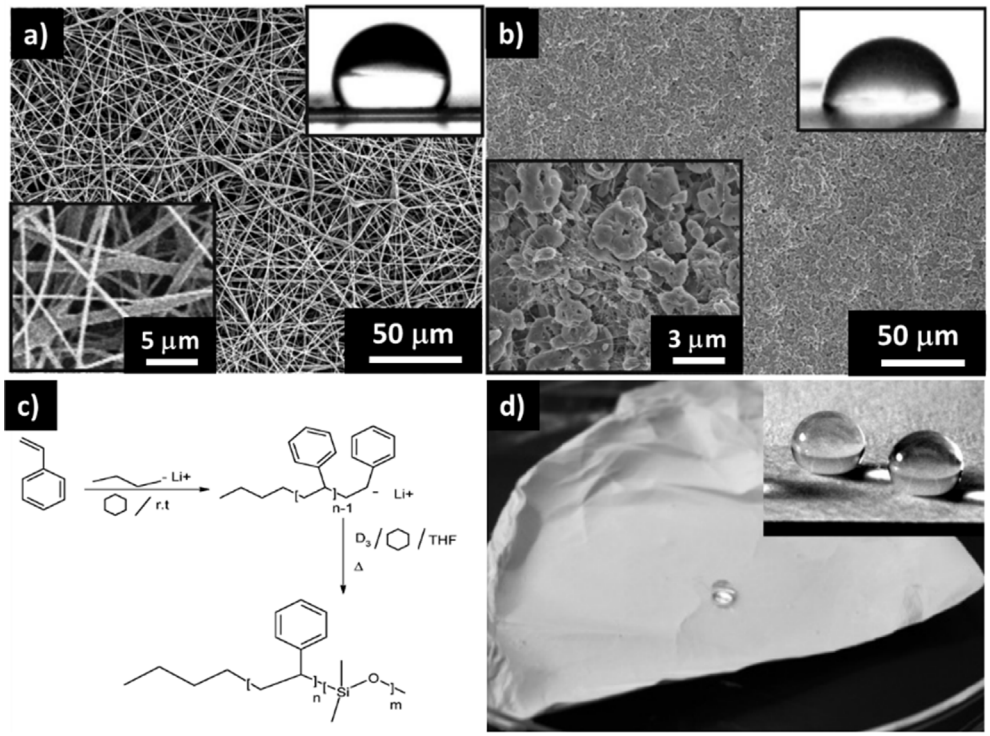

Fig. 13. a) SEM image of 17 wt% PCL electrospun fibers [160]. (b) SEM image of 1 wt% PCL electrosprayed fibre-droplet composite [160]. c) The synthesis process of PS-PDMS [161]. Reproduced with permission from [161], Copyright 2010, John Wiley and Sons. d) Superhydrophobicity of PS-PDMS/PS electrospun mat [161]. Reproduced with permission from [161], Copyright 2005, American Chemical Society.

structure. The binary system did not exhibit hydrophobicity since the water contact angle was measured as 85° on this surface (Fig. 13a and 13b) [160]. The comparisons demonstrated the superiority of electrospun nanofiber being used as a self-cleaning hydrophobic surface.

More works preferred to fabricate nanofibers with mixtures since multi-component nanofibers can process better hydrophobicity and stronger mechanical properties. Besides, some unspinnable materials with good hydrophobicity can be mixed with spinnable components for electrospinning. For instance, Ma *et al.* obtained the superhydrophobic nanofiber mats by electrospinning the co-mixtures of poly(styrene-b-dimethylsiloxane) (PDMS) blended with PS (Fig. 13c). The PDMS used in the solutions contributed the low surface tension and surface roughness to the pristine PS electrospun fibers. The WCA measured on PS-PDMS/PS nanofibrous surface was 163°. Compared with the pristine PS nanofiber hydrophobicity [159], the contact angle was enhanced by about 5.2% by hybrid nanofibers (Fig. 13d) [161]. Liu *et al.* prepared 300–400 nm diameter PI/N-methyl-2-pyrrolidone (NMP) nanofibers [162], and the contact angle measured on the 20 wt% PI/NMP nanotextured surface was 140.7°. This value was much larger than that obtained from PI powders (73° WCA) or PI/NMP film (92° WCA). Besides the electrospinning technique, the coaxial electrospinning method is also used for fabricating hydrophobic surfaces. Sun *et al.* fabricated the core–shell fibers with octadecane as the core and hydrophobic polyvinyl butyral (PVB) as the shell *via* coaxial electrospinning [163]. Han *et al.* developed superhydrophobic and oleophobic core–shell PCL/Teflon AF (amorphous fluoropolymer) nanofibers, and the corresponding contact angle was measured as 153° [164]. Adding additives, such as nanoparticles, is also an effective way to enhance the surface hydrophobicity. Sun *et al.* chose poly (vinylidene fluoride) (PVDF) mixed with silane coupling agent modified SiO_2 nanoparticles. The surface roughness and superhydrophobic property of PVDF membrane were improved by adding modified SiO_2 nanoparticles [165].

3.3.2.2. Biomimetic hydrophobic structures. The research works listed above employed the intrinsically hydrophobic mixtures as the experimental substance. Introducing natural micro- or nano-scale functional structure to the artificial materials was considered as an alternative way to gain hydrophobic properties. Some plants and insects have displayed remarkable hydrophobicity. Mimicking functional structures have been realized by several techniques. For example, Gao *et al.* developed a compound with eye-like surface structure, which was inspired by the mosquito eye structure, *via* the soft-lithography method [166]. Karaman *et al.* fabricated a self-supporting surface *via* initiated chemical vapor deposition (iCVD), which was inspired by the rose petal structure [167]. Among all methods, using the electrospinning process to manipulate fiber morphology is relatively simple and effective. So far, several bio-inspired structures have already been realized by employing the electrospinning method.

The most popular imitated object is lotus leaf (Fig. 11a). As stated, the lotus effect is caused by the hierarchical structures of the lotus surface (Fig. 11b). Developing lotus-leaf-like structures on nanofibers can enhance the fiber roughness and result in water-repellency. For example, Zhu *et al.* fabricated conducting polyaniline (PANI) and PS *via* the electrospinning method. The obtained PANI/PS composite nanofibers processed a lotus-leaf-like structure (Fig. 14a and 14b) and over 160° WCA. The functional electrospun nanofibers exhibited great superhydrophobicity in the wide pH range of 0.25 to 13.68 [168]. Similarly, Yoon *et al.* electro-sprayed PCL solutions for 2 h and obtained a fiber-droplet layer, which was usually considered as an undesirable electrospinning product. 2 h spaying resulted in lotus-leaf-like protrusions in layers. The corresponding 172° WCA was remarkably higher than 128.5° WCA of PCL nanofiber mats [160]. Kang *et al.* reported a hierarchical protuberant structure on the PS/DMF nanofibers and resulted in a higher 154.2° WCA compared with smooth PS/THF (138.1° WCA) or PS/chloroform (138.8° WCA) nanofibers [169].

The hydrophobic functional structure can also be observed on silver ragworts, honeycombs, polar bear furs, and rice leaves, *etc*. For instance, the WCA on the surface of silver ragwort leaves was 150°. Since silver ragwort leaves are covered by fibrous trichomes and numerous grooves, which is the vital structure for the hydrophobicity of artificial materials. Several works are developed based on these natural structures. Electrospun PS mats with wrinkled fiber surfaces were found to

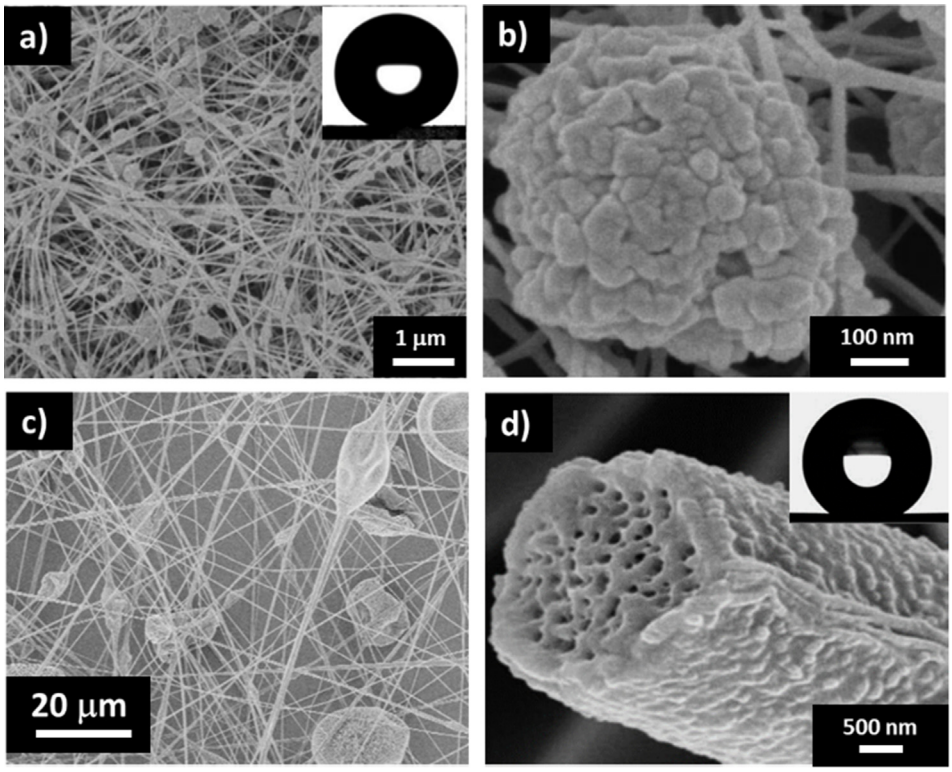

Fig. 14. a) SEM image of electrospun nanofibers with lotus-leaf-like structures [168]. b) Magnified view of Fig. 14a [168]. Reproduced with permission from [168], Copyright 2006, John Wiley and Sons. c) SEM image of a PS nanofiber with partially rose petal-like structure [171]. Reproduced with permission from [171], Copyright 2015, John Wiley and Sons. d) SEM image of fiber with cactus-like structures [172]. Reproduced with permission from [172], Copyright 2018, Royal Society of Chemistry.

present an excellent superhydrophobic property, which was inspired by the silver ragwort leaf surface structures [170]. Wong *et al.* fabricated a 3D nano-mesh *via* electrospinning PS solutions. They developed electrospun fibers with rose petal-like structures (Fig. 14c), which resulted in superhydrophobic properties (152° WCA) [171]. Zaarour *et al.* reported cactus-like nanofibers by electrospinning 22 wt% PVDF/DMF/acetone solutions. The cactus-like structure (Fig. 14d) displayed high surface superhydrophobicity (156° WCA) at 62% relative humidity (RH) [172].

3.3.2.3. Hydrophobic post-treatments to well-fabricated electrospun nanofibers. Applying post-treatments to the fabricated electrospun nanofibers is also considered as a valid option to improve hydrophobicity. Coating hydrophobic substances can effectively improve the hydrophobicity of materials. For example, electrospun CA nanofibers is a hydrophilic surface since the hydroxyl group in its formula is a hydrophilic group. The water droplets placed on the non-modified CA surface will be absorbed immediately. Ogawa *et al.* dip-coated CA membrane by immersing it into TiO_2 colloid solutions and poly (acrylic acid) (PAA) solution successively for multiple times until the layer-by-layer (LBL) films formed [173]. 10 times LBL coating introduced silver ragwort-leaf-like structures to hydrophilic nanofibers, and resulted in superhydrophobic 162° WCA on the modified surface [173]. Furthermore, Ma *et al.* produced PCL fibers (ranging from 600 nm to 2.2 μm) and coated them with hydrophobic polymerized perfluoroalkyl ethyl methacrylate (PPFEMA) *via* an iCVD method. The modification process allowed the nanofiber mats to sustain the original hierarchical surface roughness and induced advantages of low surface energy resulting from PPFEMA coating. This modification resulted in the stable surface superhydrophobicity with 175° WCA [174].

3.3.3. Self-cleaning hydrophilic electrospun nanofibers

A self-cleaning hydrophilic surface is produced mainly through spinning photocatalytic substances or post-treatments to well-fabricated nanofibers. These handling methods can introduce hydrophilic properties to fibers while the fiber themselves do not possess any functional properties. For example, cotton fibers could be dip-coated with titanium dioxide nano-colloid to gain functionalities such as self-cleaning, anti-bacteria, and decomposition of attached contaminates [175]. However, the durability of the photocatalytic coatings for some fibers is inadequate and leads to short durability and non-reusability. Thus, fabricating fibers with intrinsically hydrophilic property is quite essential.

The study of self-cleaning hydrophilic electrospun nanofibers is still in progress. Currently, fabricating hydrophilic nanofibers is mainly in two ways. One way is using hydrophilic polymers as spinning materials. Li *et al.* fabricated pristine PVDF and PVDF/PVA blended nanofibers through electrospinning technique (Fig. 15a) [176]. The average fiber diameter and porosity of the pristine PVDF membrane were measured as 1.13 μm and 85%, respectively. These pure fibers exhibited good hydrophobicity since WCA on this surface was measured as 121.1°. The hydrophilicity of this hydrophobic membrane was introduced through blending hydrophilic PVA polymers. 15 wt% PVA content in the electrospun membrane resulted in 74.5° WCA, which was tremendously reduced compared with pristine fibers [176]. Another way to improve the surface hydrophilicity is adding photocatalytic substances. Bedford and Steckl created self-cleaning photocatalytic nanofibers using a coaxial electrospinning method [177]. The obtained nanofibers (Fig. 15c and 15d) had CA as the core and TiO_2 nanoparticles as the shell. Even tested only under the room lighting condition for 24 h, the fiber mat self-cleaning progress could still be observed (Fig. 15b). Most importantly, the obtained fibers mats still sustained self-cleaning properties after several washing steps [177]. According to the photocatalytic mechanism, such phenomenon was caused by the hydroxyl radicals generated by photocatalysts during the photocatalytic progress. Therefore, this case also demonstrated that electruspun nanofibers prepared with photocatalytic additives could effectively oxidize contaminates and decompose the attached stains. Very recently, Jeong and Lee fabricated uniform PVA nanofibers blended with TiO_2 nanoparticles *via* an electrospinning method. The self-cleaning performance was tested by decomposition of methylene blue and red wine stains. Their work demonstrated that TiO_2/PVA nanofiber mats could exhibit self-

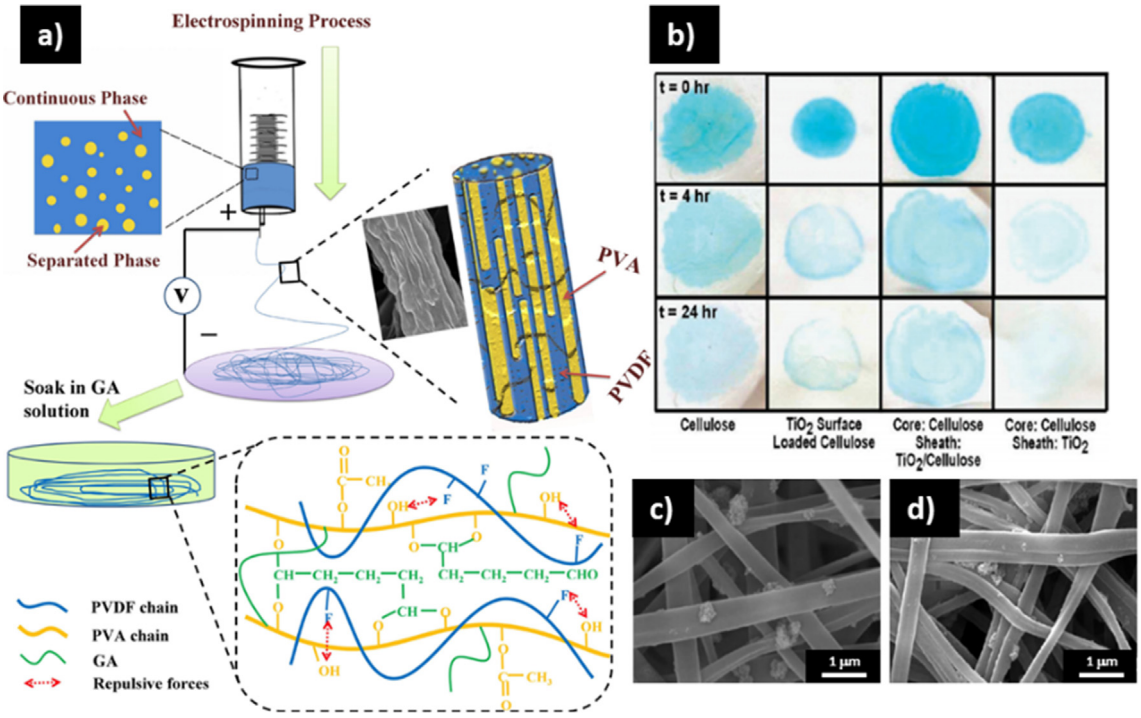

Fig. 15. a) Schematic of the preparation process for PVDF/PVA electrospun nanofibers [176]. Reproduced with permission from [176], Copyright 2020, John Wiley and Sons. b) Discoloration of Keyacid Blue stain in various species of electrospun nonwoven mats [177]. c)-d) SEM images of CA/TiO_2 core/shell nanofibers: as spun (c) and (d) post-deacetylation [177]. Reproduced with permission from [177], Copyright 2010, American Chemical Society. (For interpretation of the references to colour in this figure legend, the reader is referred to the web version of this article.)

cleaning functions under UV irradiation, visible and fluorescent light. They concluded that the decomposition rate would be enhanced by increasing light exposure time and TiO_2 concentration [178]. These experimental results demonstrated the potential usage of the electrospun nanofibers mixed with photocatalyst as improvement of the current producing progress of self-cleaning hydrophilic materials.

4. Conclusions and outlooks

The current work focuses on the fabrication of electrospun nanofibers and their environmental applications. First, we summarized the fundamental electrospinning process in three aspects including experimental setup, mechanism, and effecting parameters. Solid electrospun nanofibers have been demonstrated to be applicable in many areas, such as absorption, heat transfer, and tissue engineering. Second, three widely studied structures (core–shell, alignment, and hollow nanofibers) were summarized in the current review. The corresponding modified electrospinning process, as well as the applications, were described in detail. Finally, three environmental applications (particulate filtration, heavy metal ion removal, and self-cleaning technique) of electrospun nanofibers were discussed.

It has been widely accepted that electrospun nanofibers are promising materials used for environmental applications. However, there are still several unsolved problems of electrospun nanofibers used as filters or absorbents. First, most of the works regarding filtration or absorption were focused on using various polymers/solvents to fabricate different nanofibers and testing the corresponding filtration/absorption performance. Although experimental results obtained from these works have shown high filtration/absorption performance of electrospun nanofibers, very few lab-scale filters are applicable for large-scale industrial production. Second, the pores of electrospun nanofibers can be easily blocked by contaminates. This drawback constrains nanofibers from being used as sustainable filters or absorbents. Moreover, we have noticed that minimal amounts of researches have studied such issues. Third, poor mechanical properties and ununiformed textures make electrospun nanofibers challenging to be fully commercialized.

Furthermore, several drawbacks are found from the current researches about the self-cleaning electrospun nanofibers. First, most of the works in this area are focused on the enhancement of hydrophobic or hydrophilic properties. A limited amount of works has tested additional properties of self-cleaning nanofibers such as absorbability and permeability. Second, the current fabrication method of self-cleaning electrospun nanofibers, either hydrophobic or hydrophilic, is relatively complicated, and the self-cleaning property is not long-lasting. Longer serving life and more straightforward operating progress to obtain self-cleaning nanofibers are still highly requested.

In our opinion, the future research direction of electrospun nanofibers can be developed as follows. (i) Exploring more possibilities of using natural polymers as filtration system in the field of environmental applications. Contrary to the abundant species of additive being added to synthetic polymeric solutions and studied for the electrospinning process, more combinations of natural polymers and additives need to be tested and evaluated in the future. Besides, some natural polymers (such as chitosan) intrinsically exhibit antibacterial activities. Thus, studying air filters made from naturally polymeric electrospun nanofibers can significantly contribute to the further development of filtration system, such as odor remover and air purifier. (ii) Developing high-efficiency ultrafine particulates (UFPs) nanofibrous filters. From the perspective of urban environment, UFPs are considered as more aggressive health implications than larger PM in urban areas and the current developed air filters cannot efficiently remove such ultrafine particles. Currently, there are very few commercial products can effectively filtrate UFPs. Thus, studying electrospun nanofibers with smaller size of pore/fiber may contribute to the future development of UFPs filters. (iii) Exploring more possibilities of functional electrospun nanofibers used as biomedical nanomaterials. The field of biomedical nanomaterials is still underdeveloped. During the COVID-19 pandemic in 2020, markets are highly requesting biomaterials with better performance to cater to the increasing desires, such as materials that can

effectively remove bacteria or virus, antibacterial personal protective equipment (PPE), and wound dressings that can accelerate healing process. Thus, exploring the possibilities of electrospun nanofibers being used as biomaterials, such as new type of antibacterial PPE, absorbable surgical sutures with antibacterial functionality and novel carriers of wound healing agents, can play an essential role in the field of biomedicine and become the next possible research path. (iv) Exploring more applications of self-cleaning electrospun nanofibers. Since particles captured by self-cleaning hydrophobic surface can be removed easily via natural powers, using self-cleaning hydrophobic nanofibers as a PM filter may provide a possible method to enhance the current drawbacks of low sustainability and reusability. (v) Exploring electrospun nanofibers with enhanced mechanical properties. Poor mechanical performance is one of the most important factors that restricting electrospun nanofibers used for large-scale applications. However, the current developed enhancement methods are relatively complicated, and the mechanical performance of treated nanofibers are undesirable. Thus, developing better mechanical performance of electrospun nanofibers is still highly demanded until now. Finally, we hope this review will shed light on the future development of electrospun nanofibers and their more applications.

Declaration of Competing Interest

The authors declare that they have no known competing financial interests or personal relationships that could have appeared to influence the work reported in this paper.

Acknowledgements

We gratefully acknowledge financial support from National Natural Science Foundation of China (Grant No. 51872156).

References

[1] Krishna IM, Manickam V, Shah A, Davergave N. Environmental management: science and engineering for industry. Oxford, United Kingdom: Butterworth-Heinemann; 2017.
[2] Cisneros R, Bytnerowicz A, Schweizer D, Zhong S, Traina S. Bennett DH Ozone, nitric acid, and ammonia air pollution is unhealthy for people and ecosystems in southern Sierra Nevada. California Environ Pollut 2010;158:3261–71.
[3] Ayers GP, Gras JL. The concentration of ammonia in Southern Ocean air. J Geophys Res Oceans 1983;88:55–10659.
[4] Lindgren T. A case of indoor air pollution of ammonia emitted from concrete in a newly built office in Beijing. Build Environ 2010;45:596–600.
[5] Hexter AC, Goldsmith JR. Carbon monoxide: association of community air pollution with mortality. Science 1971;172:265–7.
[6] Raub JA, Mathieu-Nolf M, Hampson NB, Thom SR. Carbon monoxide poisoning-a public health perspective. Toxicology 2000;145:1–14.
[7] Dockery DW, Pope CA. Acute respiratory effects of particulate air pollution. Annu Rev Public Health 1994;15:107–32.
[8] Seaton A, Godden D, MacNee W, Donaldson K. Particulate air pollution and acute health effects. The Lancet 1995;345:176–8.
[9] Zhang R, Liu C, Zhou G, Sun J, Liu N, Hsu P, et al. Morphology and property investigation of primary particles from different sources. Nano Res 2018;11:3182–92.
[10] Mohammed AS, Kapri A, Goel R. Heavy metal pollution: source, impact, and remedies. Biomanagement of metal-contaminated soils. Dordrecht, Holland: Springer; 2011.
[11] Hartgerink JD, Beniash E, Stupp SI. Self-assembly and mineralization of peptide-amphiphile nanofibers. Science 2001;294:1684–8.
[12] Paramonov SE, Jun HW, Hartgerink JD. Self-assembly of peptide-amphiphile nanofibers: the roles of hydrogen bonding and amphiphilic packing. J Am Chem Soc 2006;128:7291–8.
[13] Sargeant TD, Guler MO, Oppenheimer SM, Mata A, Satcher RL, Dunand DC, et al. Hybrid bone implants: self-assembly of peptide amphiphile nanofibers within porous titanium. Biomaterials 2008;29:161–71.
[14] Ellison CJ, Phatak A, Giles DW, Macosko CW, Bates FS. Melt blown nanofibers: Fiber diameter distributions and onset of fiber breakup. Polymer 2007;48:3306–16.
[15] Hassan MA, Yeom BY, Wilkie A, Pourdeyhimi B, Khan SA. Fabrication of nanofiber meltblown membranes and their filtration properties. J Membrane Sci 2013;427:336–44.
[16] Zuo F, Tan DH, Wang Z, Jeung S, Macosko CW, Bates FS. Nanofibers from melt blown fiber-in-fiber polymer blends. ACS Macro Lett 2013;2:301–5.
[17] Sinha-Ray S, Zhang W, Sahu RP, Sinha-Ray S, Yarin AL. Pool boiling of Novec 7300 and DI water on nano-textured heater covered with supersonically-blown or electrospun polymer nanofibers. Int J Heat Mass Tran 2017;106:482–90.
[18] Sinha-Ray S, Zhang W, Stoltz B, Sahu RP, Sinha-Ray S, Yarin AL. Swing-like pool boiling on nano-textured surfaces for microgravity applications related to cooling of high-power microelectronics. npj Microgravity 2017;3:1–9.
[19] Sinha-Ray S, Zhang Y, Yarin AL, Davis SC, Pourdeyhimi B. Solution blowing of soy protein fibers. Biomacromolecules 2011;12:2357–63.
[20] Sinha-Ray S, Sinha-Ray S, Yarin AL, Pourdeyhimi B. Application of solution-blown 20–50 nm nanofibers in filtration of nanoparticles: The efficient van der Waals collectors. J Membrane Sci 2015;485:132–50.
[21] Lee MW, Yoon SS, Yarin AL. Solution-blown core–shell self-healing nano-and microfibers. ACS Appl Mater Inter 2016;8:4955–62.
[22] Subbiah T, Bhat GS, Tock RW, Parameswaran S, Ramkumar SS. Electrospinning of nanofibers. J Appl Polym 2005;96:557–69.
[23] Matthews JA, Wnek GE, Simpson DG, Bowlin GL. Electrospinning of collagen nanofibers. Biomacromolecules 2002;3:232–8.
[24] Khalid B, Bai X, Wei H, Huang Y, Wu H, Cui Y. Direct blow-spinning of nanofibers on a window screen for highly efficient PM 2.5 removal. Nano Lett 2017;17:1140–8.
[25] Wang H, Lin S, Zu D, Song J, Liu Z, Li L, et al. Direct blow spinning of flexible and transparent Ag nanofiber heater. Adv Mater Technol 2019;4:1900045.
[26] Sill TJ, von Recum HA. Electrospinning: applications in drug delivery and tissue engineering. Biomaterials 2008;29:1989–2006.
[27] Li WJ, Laurencin CT, Caterson EJ, Tuan RS, Ko FK. Electrospun nanofibrous structure: a novel scaffold for tissue engineering. J Biomed 2002;60:613–21.
[28] Pham QP, Sharma U, Mikos AG. Electrospinning of polymeric nanofibers for tissue engineering applications: A review. Tissue Eng 2006;12:1197–211.
[29] Zhang X, Reagan MR, Kaplan DL. Electrospun silk biomaterial scaffolds for regenerative medicine. Adv Drug Deliv Rev 2009;61:988–1006.
[30] Khadka DB, Haynie DT. Protein-and peptide-based electrospun nanofibers in medical biomaterials. Nanomed Nanotechnol 2012;8:1242–62.
[31] Augustine R, Malik HN, Singhal DK, Mukherjee A, Malakar D, Kalarikkal N, et al. Electrospun polycaprolactone/ZnO nanocomposite membranes as biomaterials with antibacterial and cell adhesion properties. J Polym Res 2014;21:347.
[32] Ji L, Zhang X. Electrospun carbon nanofibers containing silicon particles as an energy-storage medium. Carbon 2009;47:3219–26.
[33] Cai Y, Ke H, Dong J, Wei Q, Lin J, Zhao Y, et al. Effects of nano-SiO_2 on morphology, thermal energy storage, thermal stability, and combustion properties of electrospun lauric acid/PET ultrafine composite fibers as form-stable phase change materials. Appl Energy 2011;88:2106–12.
[34] Bonso JS, Kalaw GD, Ferraris JP. High surface area carbon nanofibers derived from electrospun PIM-1 for energy storage applications. J Mater Chem A 2014;2:418–24.
[35] Zeng J, Xu X, Chen X, Liang Q, Bian X, Yang L, et al. Biodegradable electrospun fibers for drug delivery. J Control Release 2003;92:227–31.
[36] Kenawy ER, Abdel-Hay FI, El-Newehy MH, Wnek GE. Processing of polymer nanofibers through electrospinning as drug delivery systems. Nanomaterials: Risks and Benefits. Dordrecht, Holland: Springer; 2009.
[37] Hu X, Liu S, Zhou G, Huang Y, Xie Z, Jing X. Electrospinning of polymeric nanofibers for drug delivery applications. J Control Release 2014;185:12–21.
[38] Homaeigohar S, Elbahri M. Nanocomposite electrospun nanofiber membranes for environmental remediation. Materials 2014;7:1017–45.
[39] Tian Y, Wu M, Liu R, Li Y, Wang D, Tan J, et al. Electrospun membrane of cellulose acetate for heavy metal ion adsorption in water treatment. Carbohydr Polym 2011;83:743–8.
[40] Huang Y, Miao YE, Liu T. Electrospun fibrous membranes for efficient heavy metal removal. J Appl Polym 2014:131.
[41] Formhals A. Process and apparatus for preparing artificial threads. US Patent 1975504, 1934.
[42] Chen JP, Chang GY, Chen JK. Electrospun collagen/chitosan nanofibrous membrane as wound dressing. Colloid Surf A: Physicochem Eng Asp 2008;313:183–8.
[43] Sell SA, McClure MJ, Garg K, Wolfe PS, Bowlin GL. Electrospinning of collagen/biopolymers for regenerative medicine and cardiovascular tissue engineering. Adv Drug Deliv Rev 2009;61:1007–19.
[44] Zhang YZ, Venugopal J, Huang ZM, Lim CT, Ramakrishna S. Crosslinking of the electrospun gelatin nanofibers. Polymer 2006;47:2911–7.
[45] Rujitanaroj PO, Pimpha N, Supaphol P. Wound-dressing materials with antibacterial activity from electrospun gelatin fiber mats containing silver nanoparticles. Polymer 2008;49:4723–32.
[46] Sisson K, Zhang C, Farach-Carson MC, Chase DB, Rabolt JF. Evaluation of cross-linking methods for electrospun gelatin on cell growth and viability. Biomacromolecules 2009;10:1675–80.
[47] Vega-Lugo AC, Lim LT. Electrospinning of soy protein isolate nanofibers. J Biobased Mater 2008;2:223–30.
[48] Nieuwland M, Geerdink P, Brier P, Van Den Eijnden P, Henket JT, Langelaan ML, et al. Food-grade electrospinning of proteins. Innov Food Sci Emerg Technol 2013;20:269–75.
[49] Cho D, Naydich A, Frey MW, Joo YL. Further improvement of air filtration efficiency of cellulose filters coated with nanofibers via inclusion of electrostatically active nanoparticles. Polymer 2013;54:2364–72.
[50] Desai K, Kit K, Li J, Davidson PM, Zivanovis S, Meyer H. Nanofibrous chitosan non-wovens for filtration applications. Polymer 2009;50:3661–9.
[51] Sell SA, Wolfe PS, Garg K, McCool JM, Rodriguez IA, Bowlin GL. The use of natural polymers in tissue engineering: a focus on electrospun extracellular matrix analogues. Polymer 2010;2:522–53.

[52] Mandal BK. Polymer synthesis-strategies and tactics. Darien, United States: Covalent Press, Inc; 2009.
[53] An H, Shin C, Chase GG. Ion exchanger using electrospun polystyrene nanofibers. J Membrane Sci 2006;283:84–7.
[54] Stachewicz U, Qiao T, Rawlinson SCF, Almeida FV, Li W, Cattell M, et al. 3D imaging of cell interactions with electrospun PLGA nanofiber membranes for bone regeneration. Acta Biomater 2015;27:88–100.
[55] Razzaz A, Ghorban S, Hosayni L, Irani M, Aliabadi M. Chitosan nanofibers functionalized by TiO_2 nanoparticles for the removal of heavy metal ions. J Taiwan Inst Chem E 2016;58:333–43.
[56] Yarin AL, Pourdeyhimi B, Ramakrishna S. Fundamentals and applications of micro-and nanofibers. Cambridge, England: Cambridge University Press; 2014.
[57] Zhang R, Liu C, Hsu PC, Zhang C, Liu N, Zhang J, et al. Nanofiber air filters with high-temperature stability for efficient PM 2.5 removal from the pollution sources. Nano Lett 2016;16:3642–9.
[58] Zhao R, Li X, Li Y, Li Y, Sun B, Zhang N, et al. Functionalized magnetic iron oxide/polyacrylonitrile composite electrospun fibers as effective chromium (VI) adsorbents for water purification. J Colloid Interf Sci 2017;505:1018–30.
[59] Choi HY, Bae JH, Hasegawa Y, An S, Kim IS, Lee H, et al. Thiol-functionalized cellulose nanofiber membranes for the effective adsorption of heavy metal ions in water. Carbohydr Polym 2020;115881.
[60] Zhao Y, Jie X, Xiangyang S, Ko F. Capturing cancer cells using hyaluronic acid-immobilized electrospun random or aligned PLA nanofibers. Colloid Surf A: Physicochem Eng Asp 2019;583:123978.
[61] Deitzel JM, Kleinmeyer J, Harris DEA, Tan NB. The effect of processing variables on the morphology of electrospun nanofibers and textiles. Polymer 2001;42:261–72.
[62] Wu CM, Chiou HG, Lin SL, Lin JM. Effects of electrostatic polarity and the types of electricalcharging on electrospinning behavior. J Appl Polym 2012;126:E89–97.
[63] Mazoochi T, Hamadanian M, Ahmadi M, Jabbari V. Investigation on the morphological characteristics of nanofiberous membrane as electrospun in the different processing parameters. Int J Ind Chem 2012;3:2.
[64] Beachley V, Wen X. Effect of electrospinning parameters on the nanofiber diameter and length. Mater Sci Eng C 2009;29:663–8.
[65] Zong X, Kim K, Fang D, Ran S, Hsiao BS, Chu B. Structure and process relationship of electrospun bioabsorbable nanofiber membranes. Polymer 2002;43:4403–12.
[66] Choi JS, Lee SW, Jeong L, Bae SH, Min BC, Youk JH, et al. Effect of organosoluble salts on the nanofibrous structure of electrospun poly (3-hydroxybutyrate-co-3-hydroxyvalerate). Int J Biol Macromol 2004;34:249–56.
[67] Zhao S, Wu X, Wang L, Huang Y. Electrospinning of ethyl-cyanoethyl cellulose/tetrahydrofuran solutions. J Appl Polym 2004;91:242–6.
[68] Casper CL, Stephens JS, Tassi NG, Chase DB, Rabolt JF. Controlling surface morphology of electrospun polystyrene fibers: Effect of humidity and molecular weight in the electrospinning process. Macromolecules 2004;37:573–8.
[69] Huang L, Bui N, Manickam SS, McCutcheon JR. Controlling electrospun nanofiber morphology and mechanical properties using humidity. J Polym Sci B Polym Phys 2011;49:1734–44.
[70] Nezarati RM, Eifert MB, Cosgriff-Hernandez E. Effects of humidity and solution viscosity on electrospun fiber morphology. Tissue Eng Part C ME 2013;19:810–9.
[71] De Vrieze S, Van Camp T, Nelvig A, Hagström B, Westbroek P, De Clerck K. The effect of temperature and humidity on electrospinning. J Mater Sci 2009;44:1357–62.
[72] Su Y, Lu B, Xie Y, Ma Z, Liu L, Zhao H, et al. Temperature effect on electrospinning of nanobelts: the case of hafnium oxide. Nanotechnology 2011;22:285609.
[73] Desai K, Kit K. Effect of spinning temperature and blend ratios on electrospun chitosan/poly (acrylamide) blends fibers. Polymer 2008;49:4046–50.
[74] Doshi J, Reneker DJ. Electrospinning process and applications of electrospun fibers. J Electrostat 1995;35:151–60.
[75] Bakar SSS, Fong KC, Eleyas A, Nazeri MFM. Effect of voltage and flow rate electrospinning parameters on polyacrylonitrile electrospun fibers. Mater Sci Eng 2018;318:012076.
[76] Zargham S, Bazgir S, Tavakoli A, Rashidi AS, Damerchely R. The effect of flow rate on morphology and deposition area of electrospun nylon 6 nanofiber. J Eng Fiber Fabr 2012;7. 155892501200700414.
[77] Milleret V, Simona B, Neuenschwander P, Hall H. Tuning electrospinning parameters for production of 3D-fiber-fleeces with increased porosity for soft tissue engineering applications. Eur Cells Mater 2011;21:286–303.
[78] Ding W, Wei S, Zhu J, Chen X, Rutman D, Guo Z. Manipulated electrospun PVA nanofibers with inexpensive salts. Macromol Mater Eng 2010;295:958–65.
[79] Angammana CJ, Jayaram SH. Analysis of the effects of solution conductivity on electrospinning process and fiber morphology. IEEE Trans Ind Appl 2011;47:1109–17.
[80] Haider A, Haider S, Kang I. A comprehensive review summarizing the effect of electrospinning parameters and potential applications of nanofibers in biomedical and biotechnology. Arab J Chem 2018;11:1165–88.
[81] Theron A, Zussman E, Yarin AL. Electrostatic field-assisted alignment of electrospun nanofibres. Nanotechnology 2001;12:384.
[82] Andalib MN, Lee JS, Ha L, Dzenis Y, Lim JY. Focal adhesion kinase regulation in stem cell alignment and spreading on nanofibers. Biochem Biophys Res Commun 2016;473:920–5.
[83] Katta P, Alessandro M, Ramsier RD, Chase GG. Continuous electrospinning of aligned polymer nanofibers onto a wire drum collector. Nano Lett 2004;4:2215–8.
[84] Zhao J, Liu H, Lan Xu. Preparation and formation mechanism of highly aligned electrospun nanofibers using a modified parallel electrode method. Eng Mater Des 2016;90:1–6.
[85] Liu J, Chen G, Hui G, Zhang L, Ma S, Liang J, et al. Structure and thermo-chemical properties of continuous bundles of aligned and stretched electrospun polyacrylonitrile precursor nanofibers collected in a flowing water bath. Carbon 2012;50:1262–70.
[86] Savva I, Evaggelou E, Papaparaskeva G, Leontiou T, Stylianopoulos T, Mpekris F, et al. Alignment of electrospun polymer fibers using a concave collector. RSC Adv 2015;5:104400.
[87] Yang Y, Jia Z, Li Q, Wang L, Guan Z. Improving electrospinning nanofibers alignment in a large area by using a insulating tube on the collector. IEEE ICSD 2007:419–22.
[88] Sun D, Chang C, Li S, Lin L. Near-field electrospinning. Nano Lett 2006;6:839–42.
[89] Zheng G, Li W, Wang X, Wu D, Sun D, Lin L. Precision deposition of a nanofibre by near-field electrospinning. J Phys D: Appl Phys 2010;43:415501.
[90] Brown TD, Dalton PD, Hutmacher DW. Direct writing by way of melt electrospinning. Adv Mater 2011;23:5651–7.
[91] Edmondson D, Cooper A, Jana S, Wood D, Zhang M. Centrifugal electrospinning of highly aligned polymer nanofibers over a large area. J Mater Chem 2012;22:18646.
[92] Erickson AE, Edmondson D, Chang F, Wood D, Gong A, Levengood SL, et al. High-throughput and high-yield fabrication of uniaxially-aligned chitosan-based nanofibers by centrifugal electrospinning. Carbohydr Polym 2015;134:467–74.
[93] Mei L, Song P, Liu Y. Magnetic-field-assisted electrospinning highly aligned composite nanofibers containing well-aligned multiwalled carbon nanotubes. J Appl Polym 2015;132:41995.
[94] Lee MW, An S, Lee C, Liou M, Yarin AL, Yoon SS. Self-healing transparent core—shell nanofiber coatings for anti-corrosive protection. J Mater Chem A 2014;2:7045–53.
[95] Mickova A, Buzgo M, Benada O, Rampichova M, Fisar Z, Filova E, et al. Core/shell nanofibers with embedded liposomes as a drug delivery system. Biomacromolecules 2012;13:952–62.
[96] Sun Z, Zussman E, Yarin AL, Wendorff JH, Greiner A. Compound core-shell polymer nanofibers by co-electrospinning. Adv Mater 2003;15:1929–32.
[97] Wei Q, editor. Functional nanofibers and their applications. Cambridge, England: Woodhead Publishing; 2012.
[98] Jalaja K, Naskar D, Kundu SC, James NR. Potential of electrospun core-shell structured gelatin-chitosan nanofibers for biomedical applications. Carbohydr Polym 2016;136:1098–107.
[99] Chen H, Wang N, Di J, Zhao Y, Song Y, Jiang L. Nanowire-in-microtube structured core/shell fibers via multifluidic coaxial electrospinning. Langmuir 2010;26:11291–6.
[100] Zhao Y, Cao X, Jiang L. Bio-mimic multichannel microtubes by a facile method. J Am Chem Soc 2007;129:764–5.
[101] Chen F, Huang P, Mo X. Electrospinning of heparin encapsulated P(LLA-CL) core/shell nanofibers. Nano Biomed Eng 2010;2:56–60.
[102] Khajavi R, Abbasipour M. Electrospinning as a versatile method for fabricating coreshell, hollow and porous nanofibers. Sci Iran F 2012;19:2029–34.
[103] Ouyang W, Liua S, Yao K, Zhao Lu, Cao L, Jiang S, et al. Ultrafine hollow TiO_2 nanofibers from core-shell composite fibers and their photocatalytic properties. Compos Commun 2018;9:76–80.
[104] Cui Q, Dong X, Wang J, Li M. Direct fabrication of cerium oxide hollow nanofibers by electrospinning. J Rare Earth 2008;26:664–9.
[105] Li D, Xia Y. Direct fabrication of composite and ceramic hollow nanofibres by electrospinning. Nano Lett 2004;4:933–8.
[106] Gao Q, Luo J, Wang X, Gao C, Ge M. Novel hollow α-Fe_2O_3 nanofibers via electrospinning for dye adsorption. Nanoscale Res Lett 2015;10:1–8.
[107] Tie Y, Ma SY, Pei ST, Zhang QX, Zhu KM, Zhang R, et al. Pr doped $BiFeO_3$ hollow nanofibers via electrospinning method as a formaldehyde sensor. Sensor Actuat B Chem 2020;308:127689.
[108] Chang G, Zheng X, Chen R, Chen X, Chen L, Chen Z. Silver nanoparticles filling in TiO2 hollow nanofibers by coaxial electrospinning. Acta Phys-Chim Sin 2008;24:1790–7.
[109] Ding B, Wang X, Yu J, editors. Electrospinning: Nanofabrication and applications; Norwich. William Andrew: United States; 2018.
[110] Kadam VV, Wang L, Padhye R. Electrospun nanofiber materials to filter air pollutants-A review. J Ind Text 2018;47:2253–80.
[111] Balgis R, Kartikowati CW, Ogi T, Gradon L, Bao L, Seki K, et al. Synthesis and evaluation of straight and bead-free nanofibers for improved aerosol filtration. Chem Eng Sci 2015;137:947–54.
[112] Yun KM, Suryamas AB, Iskandar F, Bao L, Niinuma H, Okuyama K. Morphology optimization of polymer nanofiber for applications in aerosol particle filtration. Sep Purif Technol 2010;75:340–5.
[113] Wang Z, Zhao C, Pan Z. Porous bead-on-string poly (lactic acid) fibrous membranes for air filtration. J Colloid Interf Sci 2015;441:121–9.
[114] Hung CH, Leung WWF. Filtration of nano-aerosol using nanofiber filter under low Peclet number and transitional flow regime. Sep Purif Technol 2011;79:34–42.
[115] Leung WWF, Hung CH, Yuen PT. Effect of face velocity, nanofiber packing density and thickness on filtration performance of filters with nanofibers coated on a substrate. Sep Purif Technol 2010;71:30–7.
[116] Zhu M, Han J, Wang F, Shao W, Xiong R, Zhang Q, et al. Electrospun nanofibers membranes for effective air filtration. Macromol Mater Eng 2017;302:1600353.
[117] Kim GT, Ahn YC, Lee JK. Characteristics of Nylon 6 nanofilter for removing ultrafine particles. Korean J Chem Eng 2008;25:368–72.
[118] Matulevicius J, KLiucininkas L, Prasauskas T, Buivydiene D, Martuzevicius D. The comparative study of aerosol filtration by electrospun polyamide, polyvinyl acetate, polyacrylonitrile and cellulose acetate nanofiber media. J. Aerosol Sci. 2016;92:27–37.
[119] Xu J, Liu C, Hsu P, Liu K, Zhang R, Liu Y, et al. Roll-to-roll transfer of electrospun

nanofiber film for high-efficiency transparent air filter. Nano Lett 2016;16:1270–5.
[120] Zatz JL, Knowles B. Effect of pH on monolayers of cellulose acetate phthalate. J Pharm Sci 1970;59:1750–1.
[121] Nicosia A, Keppler T, Muller FA, Vazquez B, Ravegnani F, Monticelli P, et al. Cellulose acetate nanofiber electrospun on nylon substrate as novel composite matrix for efficient, heat-resistant, air filters. Chem Eng Sci 2016;153:284–94.
[122] Yu Y, Ma Q, Zhang JB, Liu GB. Electrospun SiO_2 aerogel/polyacrylonitrile composited nanofibers with enhanced adsorption performance of volatile organic compounds. Appl Surf Sci 2020;145697.
[123] Wan H, Wang N, Yang J, Si Y, Chen K, Ding B, et al. Hierarchically structured polysulfone/titania fibrous membranes with enhanced air filtration performance. J Colloid Interf Sci 2014;417:18–26.
[124] Kayaci F, Uyar T. Electrospun polyester/cyclodextrin nanofibers for entrapment of volatile organic compounds. Polym Eng Sci 2014;54:2970–8.
[125] Uyar T, Havelund R, Nur Y, Hacaloglu J, Besenbacher F, Kingshott P. Molecular filters based on cyclodextrin functionalized electrospun fibers. J Membrane Sci 2009;332:129–37.
[126] Zhang R, Liu B, Yang A, Zhu Y, Liu C, Zhou G, et al. In-situ investigation on the nanoscale capture and evolution of aerosols on nanofibers. Nano Lett 2018;18:1130–8.
[127] Gautam RK, Sharma SK, Mahiya S, Chattopadhyaya MC. Contamination of heavy metals in aquatic media: transport, toxicity and technologies for remediation. R Soc Chem 2014:1–24.
[128] He T, Feng X, Guo Y, Qiu G, Li Z, Liang L, et al. The impact of eutrophication on the biogeochemical cycling of mercury species in a reservoir: a case study from Hongfeng Reservoir, Guizhou. China Environ Pollut 2008;154:56–67.
[129] Tian T, Wu M, Liu R, Li Y, Wang D, Tan J, et al. Electrospun membrane of cellulose acetate for heavy metal ion adsorption in water treatment. Carbohydr Polym 2010;82:743–8.
[130] Zhang W, Vilensky R, Zussman E, Yarin AL. Adsorption and mass transfer in granular porous membranes/media due to inserted volatile materials. Int J Heat Mass Transf 2018;116:248–58.
[131] Kongsuwan A, Patnukao P, Pavasant P. Binary component sorption of Cu (II) and Pb (II) with activated carbon from Eucalyptus camaldulensis Dehn bark. J Ind Eng Chem 2009;15:465–70.
[132] Karthikeyan T, Rajgopal S, Miranda LR. Chromium (VI) adsorption from aqueous solution by Hevea Brasilinesis sawdust activated carbon. J Hazard Mater 2005;124:192–9.
[133] Deliyanni EA, Kyzas GZ, Triantafyllidis KS, Matis KA. Activated carbons for the removal of heavy metal ions: A systematic review of recent literature focused on lead and arsenic ions. Open Chem 2015;13:699–708.
[134] Choi HJ, Yu SW, Kim KH. Efficient use of Mg-modified zeolite in the treatment of aqueous solution contaminated with heavy metal toxic ions. J Taiwan Inst Chem E 2016;63:482–9.
[135] Burakov AE, Galunin EV, Burakova IV, Kucherova AE, Agarwal S, Tkachev AG, et al. Adsorption of heavy metals on conventional and nanostructured materials for wastewater treatment purposes: A review. Ecotox Environ Safe 2018;148:702–12.
[136] Haddad MY, Alharbi HF. Enhancement of heavy metal ion adsorption using electrospun polyacrylonitrile nanofibers loaded with ZnO nanoparticles. J Appl Polym 2019;136:47209.
[137] Wu S, Li F, Wang H, Fu L, Zhang B, Li G. Effects of poly(vinyl alcohol) (PVA) content on preparation of novel thiol-functionalized mesoporous PVA/SiO_2 composite nanofiber membranes and their application for adsorption of heavy metal ions from aqueous solution. Polymer 2010;51:6203–11.
[138] Haider S, Park S. Preparation of the electrospun chitosan nanofibers and their applications to the adsorption of Cu (II) and Pb (II) ions from an aqueous solution. J Membrane Sci 2009;328:90–6.
[139] Choi J, Ide A, Truong YB, Kyratzis IL, Caruso RA. High surface area mesoporous titanium–zirconium oxide nanofibrous web: a heavy metal ion adsorbent. J Mater Chem A 2013;1:5847–53.
[140] Stephen M, Catherine N, Brenda M, Andrew K, Leslie P, Corrine G. Oxolane-2, 5-dione modified electrospun cellulose nanofibers for heavy metals adsorption. J Hazard Mater 2011;192:922–7.
[141] Feng Q, Wu D, Zhao Y, Wei A, Wei Q, Fong H. Electrospun AOPAN/RC blend nanofiber membrane for efficient removal of heavy metal ions from water. J Hazard Mater 2018;344:819–28.
[142] Shi S, Xu C, Wang X, Xie Y, Wang Y, Dong Q, et al. Electrospinning fabrication of flexible Fe_3O_4 fibers by sol-gel method with high saturation magnetization for heavy metal adsorption. Mater Des 2020;186:108298.
[143] Bornillo KAS, Kim S, Choi H. Cu (II) removal using electrospun dual-responsive polyethersulfone-poly (dimethyl amino) ethyl methacrylate (PES-PDMAEMA) blend nanofibers. Chemosphere 2020;242:125287.
[144] Law KY. Highly wettable slippery surfaces: Self-cleaning effect and mechanism. Int J Wettability Sci Technol 2018;1:31–45.
[145] Sethi SK, Manik G. Recent progress in super hydrophobic/hydrophilic self-cleaning surfaces for various industrial applications: A review. Polym Plast Technol Eng 2018;57:1932–52.
[146] Ensikat HJ, Ditsche-Kuru P, Neinhuis C, Barthlott W. Superhydrophobicity in perfection: the outstanding properties of the lotus leaf. Beilstein J Nanotechnol 2011;2:152–61.
[147] Zhang M, Feng S, Wang L, Zheng Y. Lotus effect in wetting and self-cleaning. Biotribology 2016;5:31–43.
[148] Dalrymple OK, Stefanakos E, Trotz MA, Goswami DY. A review of the mechanisms and modeling of photocatalytic disinfection. Appl Catal B- Environ 2010;98:27–38.
[149] Tung WS, Daoud WA. Self-cleaning fibers via nanotechnology: a virtual reality. J Mater Chem 2011;21:7858–69.
[150] Zhang J, Tian B, Wang L, Xing M, Lei J. Photocatalysis: fundamentals, materials and applications. Singapore: Springer; 2018.
[151] Chen X, Shen S, Guo L, Mao SS. Semiconductor-based photocatalytic hydrogen generation. Chem Rev 2010;110:6503–70.
[152] Damodar RA, You S, Chou H. Study the self cleaning, antibacterial and photocatalytic properties of TiO_2 entrapped PVDF membranes. J Hazard Mater 2009;172:1321–8.
[153] Euvananont C, Junin C, Inpor K, Limthongkul P, Thanachayanont C. TiO_2 optical coating layers for self-cleaning applications. Ceram Int 2008;34:1067–71.
[154] Onar N, Aksit AC, Sen Y, Mutlu M. Antimicrobial, UV-protective and self-cleaning properties of cotton fabrics coated by dip-coating and solvothermal coating methods. Fiber Polym 2011;12:461–70.
[155] Latthe SS, Sudhagar P, Ravidhas C, Christy AJ, Kirubakaran DD, Venkatesh R, et al. Self-cleaning and superhydrophobic CuO coating by jet-nebulizer spray pyrolysis technique. CrystEngComm 2015;17:2624–8.
[156] Benedix R, Dehn F, Quaas J, Orgass M. Application of titanium dioxide photocatalysis to create self-cleaning building materials. Lacer 2000;5:157–68.
[157] Bahgat Radwan A, Abdullah AM, Mohamed A, Al-Maadeed MA. New electrospun polystyrene/Al_2O_3 nanocomposite superhydrophobic coatings; synthesis, characterization, and application. Coatings 2018;8:65.
[158] Dalawai SP, Aly MAS, Latthe SS, Xing R, Sutar RS, Nagappan S, et al. Recent advances in durability of superhydrophobic self-cleaning technology: A critical review. Prog Org Coat 2020;138:105381.
[159] Lee MW, An S, Latthe SS, Lee C, Hong S, Yoon SS. Electrospun polystyrene nanofiber membrane with superoleophobicity and superhydrophilicity for selective of water and low viscous oil. ACS Appl Mater Inter 2013;5:10597–604.
[160] Yoon H, Park JH, Kim GH. A superhydrophobic surface fabricated by an electrostatic process. Macromol Rapid Commun 2010;31:1435–9.
[161] Ma M, Hill RM, Lowery JL, Fridrikh SV, Rutledge GC. Electrospun poly (styrene-block-dimethylsiloxane) block copolymer fibers exhibiting superhydrophobicity. Langmuir 2005;21:5549–54.
[162] Liu J, Huang J, Wujcik EK, Qiu B, Rutman D, Zhang X, et al. Hydrophobic electrospun polyimide nanofibers for self-cleaning materials. Macromol Mater Eng 2015;300:358–68.
[163] Sun SX, Xie R, Wang XX, Wen GQ, Liu Z, Wang W, et al. Fabrication of nanofibers with phase-change core and hydrophobic shell, via coaxial electrospinning using nontoxic solvent. J Mater Sci 2015;50:5729–38.
[164] Han D, Steckl AJ. Superhydrophobic and oleophobic fibers by coaxial electrospinning. Langmuir 2009;25:9454–62.
[165] Sun H, Xu Y, Zhou Y, Gao W, Zhao H, Wang W. Preparation of superhydrophobic nanocomposite fiber membranes by electrospinning poly (vinylidene fluoride)/silane coupling agent modified SiO_2 nanoparticles. J Appl Polym 2017;134:44501.
[166] Gao X, Yan X, Yao XX, Xu L, Zhang K, Zhang J, et al. The dry-style antifogging properties of mosquito compound eyes and artificial analogues prepared by soft lithography. Adv Mater 2007;19:2213–7.
[167] Karaman M, Çabuk N, Özyurt D, Köysüren Ö. Self-supporting superhydrophobic thin polymer sheets that mimic the nature's petal effect. Appl Surf Sci 2012;259:542–6.
[168] Zhu Y, Zhang J, Zheng Y, Huang Z, Feng L, Jiang L. Stable, superhydrophobic, and conductive polyaniline/polystyrene films for corrosive environments. Adv Funct Mater 2006;16:568–74.
[169] Kang M, Jung R, Kim HS, Jin HJ. Preparation of superhydrophobic polystyrene membranes by electrospinning. Colloid Surf A: Physicochem Eng Asp 2008;313:411–4.
[170] Miyauchi Y, Ding B, Shiratori S. Fabrication of a silver-ragwort-leaf-like superhydrophobic micro/nanoporous fibrous mat surface by electrospinning. Nanotechnology 2006;17:5151.
[171] Wong WSY, Nasiri N, Liu G, Rumsey-Hill N, Craig VSJ, Nisbet DR, et al. Flexible transparent hierarchical nanomesh for rose petal-like droplet manipulation and lossless transfer. Adv Mater Interfaces 2015;2:1500071.
[172] Zaarour B, Zhu L, Jin X. Fabrication of a polyvinylidene fluoride cactus-like nanofiber through one-step electrospinning. RSC Adv 2018;8:42353.
[173] Ogawa T, Ding B, Sone Y, Shiratori S. Super-hydrophobic surfaces of layer-by-layer structured film-coated electrospun nanofibrous membranes. Nanotechnology 2007;18:165607.
[174] Ma M, Mao Y, Gupta M, Gleason KK, Rutledge GC. Superhydrophobic fabrics produced by electrospinning and chemical vapor deposition. Macromolecules 2005;38:9742–8.
[175] Daoud WA, Xin JH. Nucleation and growth of anatase crystallites on cotton fabrics at low temperatures. J Am Ceram Soc 2004;87:953–5.
[176] Li M, Li J, Zhou M, Xian Y, Shui Y, Wu M, et al. Super-Hydrophilic electrospun PVDF/PVA-blended nanofiber membrane for microfiltration with ultrahigh water flux. J Appl Polym 2020;137:48416.
[177] Bedford NM, Steckl AJ. Photocatalytic self-cleaning textile fibers by coaxial electrospinning. ACS Appl Mater Inter 2010;2:2448–55.
[178] Jeong T, Lee S. Photocatalytic self-cleaning by nanocomposite fibers containing titanium dioxide nanoparticles. Fiber Polym 2019;20:25–34.